

2011

Proof-of-Concept Experiments of Hydrogen Generation by Solar Water Splitting by Using III-Nitride Alloys

Takahiro Toma
Lehigh University

Follow this and additional works at: <http://preserve.lehigh.edu/etd>

Recommended Citation

Toma, Takahiro, "Proof-of-Concept Experiments of Hydrogen Generation by Solar Water Splitting by Using III-Nitride Alloys" (2011). *Theses and Dissertations*. Paper 1290.

This Thesis is brought to you for free and open access by Lehigh Preserve. It has been accepted for inclusion in Theses and Dissertations by an authorized administrator of Lehigh Preserve. For more information, please contact preserve@lehigh.edu.

**Proof-of-Concept Experiments of Hydrogen Generation by Solar Water
Splitting by Using III-Nitride Alloys**

By

Takahiro Toma

A Thesis

Presented to the Graduate and Research Committee

of Lehigh University

in Candidacy for the Degree of

Master of Science

in

Electrical Engineering

Lehigh University

May 2011

This thesis is accepted and approved in partial fulfillment of the requirements for the Master of Science

Date

Prof. Nelson Tansu - Thesis Advisor

Prof. Filbert J. Bartoli – ECE Department Chair

Acknowledgement

It is a pleasure to thank the many people who made this thesis possible. It is difficult to overstate my gratitude to my adviser, Prof. Nelson Tansu for his motivation, enthusiasm, and immense knowledge. I could not have imagined having a better advisor and mentor for my master's study.

I would like to thank Dr. Norm Zheng (Director of Instrumentation in Department of Chemistry at Lehigh University) for the Gas Chromatography training. My sincere thanks also goes to our COT cleanroom manager Anthony Jeffers for the cleanroom training and cleanroom equipment maintenance. I would like to express my sincere gratitude to our past post-doctoral scientist Dr. Gensheng Huang (currently MOCVD Engineer at Aixtron, Inc) and present postdoctoral research fellow Dr. Renbo Song, and I have learnt a lot from them. I also would like to express my sincere gratitude to my research mates for their assistance during my master's studies at Lehigh: Dr. Yik-Khoon Ee (Philips Lumileds), Prof. Hongping Zhao (Case Western Reserve University), Dr. Hua Tong (MOCVD Scientist at Valence Process Equipment (VPE), Inc.), Guangyu Liu, Xiao-Hang Li, Jing Zhang, Vincent Handara, Tidapan Sursattayawong, Nan-Lung Wu, Joseph B. Mulhern, Shaofei Zhang, Samuel G. Wheeler, Le Zhao, Kanokwan Klinieam, Songul Kutlu, and Chongzhao Wu. I am very proud to be part of the team with them. I would also like to acknowledge Allyson K. Glazier for helpful reading of the manuscript.

I would like to thank my company USHIO inc. for the opportunity and financial support of this study in Lehigh, in particular, for the support from Corporate Senior Vice

President Tatsushi Igarashi, Corporate Vice President Akihiko Sugitani, Deputy General Manager Kensuke Fukushima, and Director of Optical Design Section Yoshio Okazaki.

Lastly, and most importantly, I would like to thank my family members for the sacrifice and understanding during my pursuit of graduate studies at Lehigh University. I am deeply indebted to my parents and sister for raising and educating me to be the person who I am today. I wish to thank my wife Rumi Toma and my lovable son Shujiro Toma, who have accompanied me with strong dedication and understanding during the pursuit of knowledge at Lehigh. They supported me, encouraged me and loved me. To my family, I dedicate this thesis.

Table of Contents

Abstract	1
Chapter 1 : Introduction	3
1.1 Background and motivation.....	3
1.2 Review of current work	5
1.3 Thesis organization.....	7
Reference for chapter 1	7
Chapter 2 : Basic Principle of Solar Water Splitting	10
2.1 Introduction of solar water splitting	10
2.2 Chemical reaction mechanism in the cell	11
2.3 Band structure.....	13
2.4 Decomposition of semiconductor	20
2.5 Efficiency of a PEC cell	22
Reference for chapter 2.....	23
Chapter 3 : Demonstration of Solar Water Splitting Employing GaN and InGaN Alloy	25
3.1 Sample Preparation for the working electrode	25
3.2 Set up for the experiment.....	26
3.3 Results of the experiment	30
3.4 Summary of the experimental work	47
Reference for chapter 3.....	47
Chapter 4 : Summary and Future Work	49
4.1 Conclusion	49
Reference for chapter 4.....	51
Curriculum Vitae.....	52

Abstract

Presently, most of the energy is generated from fossil fuel, which results in CO₂ emissions and not infinite. In order for achieving sustainable life, renewable source of energy must be found and developed. Solar water splitting is one of the candidates, as this process only requires the use of solar energy and inexhaustible water available on the earth. Moreover, exclusive by-product of the use of hydrogen technology is water. Enormous efforts have been used to pursue the use of various technologies to achieve efficient solar water splitting. However, this solar water splitting technology is still far from other dominant energy sources attributed to the difficult requirements for obtaining working electrode with desirable properties. The desired properties of the working electrodes require the need of high corrosive resistance, suitable band gap, and appropriate band edge positions for enabling the water splitting process. To address this limitation, InGaN alloy is investigated as one of the key materials for achieving electrodes suitable for solar water splitting. Band positions of the InGaN in the context of the hydrogen and oxygen redox potential are found as suitable, and band gap energy of this alloy can be adjusted by varying the In-content. In addition, InGaN has high corrosion resistivity due to the small lattice constant of the alloy, due to the stability of this alloy in aqueous solution from the strong inter-atomic bonding. Nevertheless, there has been very few research works performed on this InGaN alloy for solar water splitting experiments. In this thesis, basic principle of the solar water splitting is presented with current research on GaN and InGaN for the photo-electrode in the PEC cell. Preliminary experimental demonstrations of the solar water splitting process by employing the III-

Nitride alloys are also presented, and the results showed promising nitride semiconductors alloys for solar water splitting applications.

Chapter 1 : Introduction

1.1 Background and motivation

Solar water splitting employing semiconductor material is one of the candidates of energy sources for sustainable life. It consumes water and solar energy to generate hydrogen [1] and there is no emission of hazardous by-products. Minimal construction of the cell for the solar water splitting basically consists of two electrodes and an electrolyte. One of the electrodes should be made of semiconductor material, which is referred to as the working electrode, and the other electrode can be made of another kind of semiconductor material or metal which is referred to as the counter electrode. Upon illumination of the working electrode, electron-hole pairs are generated on the semiconductor surface and decompose water into hydrogen and oxygen. Although many semiconductor materials are capable of decomposing water with an applied bias voltage, there are a few materials, which can be employed as the working electrode in the cell and can decompose water without an applied bias voltage, due to the following requirements for a working electrode material. Firstly, the material must have chemical inertness in an aqueous electrolyte solution. In the most cases, a strong acid or a strong base solution is applied as the electrolyte in this cell. For that reason, materials that react with the electrolyte cannot be employed as the working electrode, especially in long term usage due to corrosion. Second, the material should have the suitable band gap energy for the solar spectrum. A high absorption rate of photons from the solar spectrum is required to convert energy into formation of electron-hole pairs which decompose water. Lastly, the material must have appropriate band edge positions. The conduction band edge should be

higher than the redox potential of hydrogen and the valance band edge should be lower than the redox potential of oxidation of water. The details are described in reference 9 and 11. Consequently, there are a few materials that can be employed as the working electrode in the cell and none yet fulfill all of these requirements. For instance, several oxide semiconductors, such as TiO_2 and SnO_2 , have high chemical inertness. However, their band gap energies are too large. Regarding TiO_2 , it can absorb solar light with energy of equal to or greater than 3.2eV [7], which is the band gap energy. As a result, TiO_2 can absorb less than 3% of the total solar energy and the rest of energy cannot be used for generation of electron-hole pairs. Figure 1.1 shows the solar spectrum. By contrast, GaAs and GaAsPN have appropriate band gap energies of 1.4eV [9] and 1.8eV (2.7% of N) [10], respectively. Nevertheless, these materials are corrosive in an aqueous solution. Accordingly, these materials are also not favorable candidates for the working electrode.

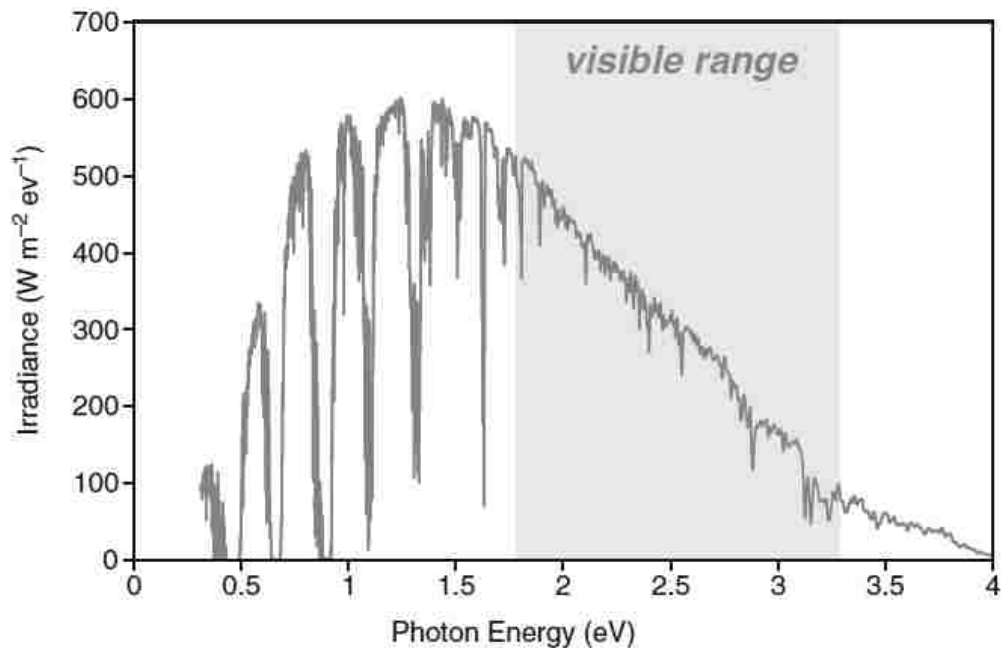


Figure 1.1. The solar spectrum AM1.5 shown as a function of photon energy [11].

Although InGaN alloy shows promising potential as the working electrode material, there have been very few research works performed with this alloy for solar water splitting. Consequently, the objective of this work is to set up the experimental apparatus to investigate water solar splitting employing III-nitride alloys, as well as to perform proof-of-concept experiments to demonstrate the feasibility of hydrogen generation from the solar water splitting in III-nitride semiconductors.

1.2 Review of current work

Applying a high In-content n-type $\text{In}_x\text{Ga}_{1-x}\text{N}$ ($x=0.4$) alloy to a PEC cell has been reported by J. Li *et al* [3]. The results demonstrated a strong dependency of photo-current and hydrogen generation rate on In-content of the InGaN alloy [3].

Solar water splitting by a high In-content p- $\text{In}_x\text{Ga}_{1-x}\text{N}$ ($x=0.22$) alloy has been demonstrated to enhance the solar light absorption rate and to obtain high chemical resistant material. This research showed the working electrode made of p-InGaN alloy generated a much higher photo-current than that of the working electrode made of p-GaN alloy. Moreover, the p-InGaN electrode is significantly more stable in the strong acid HBr, as there was no etching effect on the p-InGaN layer for twenty-four hours [4].

A patterned metal electrode on a GaN alloy for solar water splitting has been developed. Metal stripes deposited on the GaN alloy enhanced electron extraction rate from the GaN alloy [2, 8]. Direct hydrogen generation upon UV irradiation in aqueous NaOH solution was observed by Waki and co-workers [2].

Another nitride semiconductor, AlGaN, has been employed as the working electrode for the PEC cell. The results showed that band edge positions compared with the redox potentials of the hydrogen and oxidation of water were appropriate; however, the hydrogen generation rate was lower than that of the InGaN alloy owing to a larger band gap in the AlGaN alloy [5].

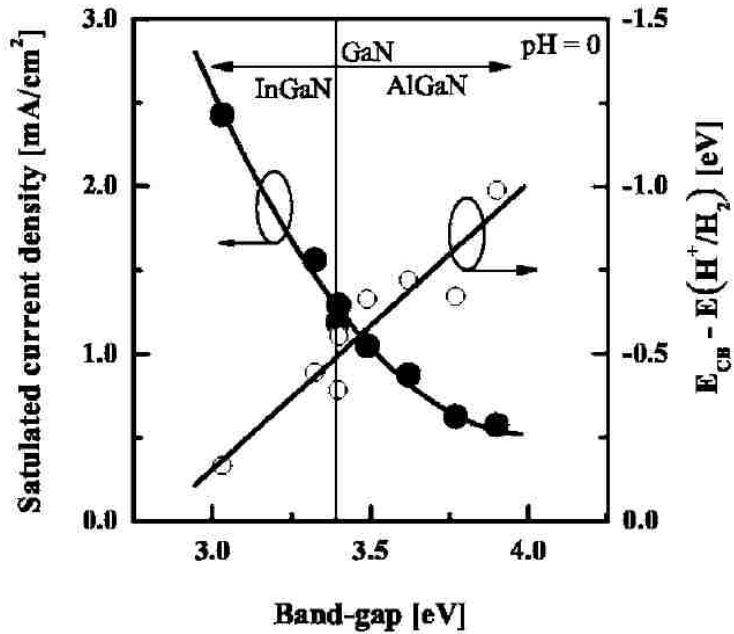


Figure 1.2. Saturated current density as a function of Band gap. Saturated current density was obtained at 1.5V for AlGaN and at 2.0V for InGaN with respect to the Ag/AgCl reference electrode. The electric potential was used as -0.212V vs normal hydrogen electrode [5].

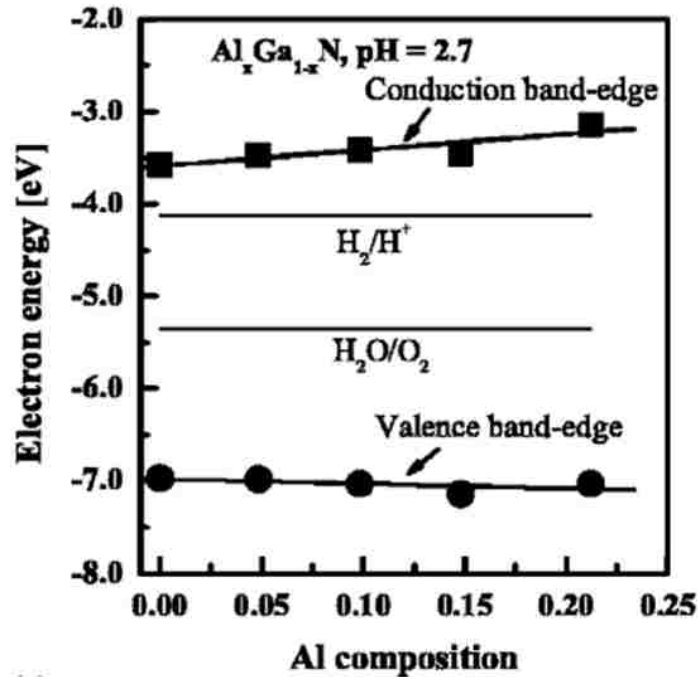


Figure 1.3. Band edge positions as a function of Al composition of $\text{Al}_x\text{Ga}_{1-x}\text{N}$ in the solution of pH 2.7 [5].

1.3 Thesis organization

The motivation of this thesis is to explain fundamental principle of the solar water splitting employing a semiconductor material as the working electrode. Additionally, the experimental setup and demonstrated results will be explained. The proof-of-concept experimental demonstration of the solar water splitting by employing GaN and InGaN based alloys will be presented.

Reference for chapter 1

- [1] A. Fujishima, K. Honda. "Electrochemical Photolysis of Water at a Semiconductor Electrode." *Nature (London)* 238, 1972: 37.

- [2] Ichitaro. Waki, Daniel Cohen, Rakesh Lal, Umesh Mishra, Steven P. DenBaars and Shuji Nakamura. "Direct water photoelectrolysis with patterned n-GaN." *Applied Physics Letters* 91, 2007: 093519.
- [3] J. Li, J. Y. Lin, and H. X. Jiang. "Direct hydrogen gas generation by using InGaN epilayers as working electrodes." *Applied Physics Letters* 93, 2008: 162107.
- [4] K. Aryal, B. N. Pantha, J. Li, J. Y. Lin, and H. X. Jiang. "Hydrogen generation by solar water splitting using p-InGaN photoelectrochemical cells." *Applied Physics Letters* 96, 2010: 052110.
- [5] Katsushi Fujii, Masato Ono, Takashi Ito, Yasuhiro Iwaki, Akira Hirako and Kazuhiro Ohkawa. "Band-Edge Energies and Photoelectrochemical Properties of n-Type $\text{Al}_x\text{Ga}_{1-x}\text{N}$ and $\text{In}_y\text{Ga}_{1-y}\text{N}$ Alloys." *Journal of The Electrochemical Society*, 154 (2), 2007: B175-B179.
- [6] Muhammad Jamil, Hongping Zhao, John B. Higgins, and Nelson Tansu. "MOVPE and photoluminescence of narrow band gap (0.77 eV) InN on GaN/sapphire by pulsed growth mode." *phys. stat. sol. (a)* 205, No. 12, 2008: 2886-2891.
- [7] Nobuyuki Sakai, Yasuo Ebina, Kazunori Takada, and Takayoshi Sasaki. "Electronic Band Structure of Titania Semiconductor Nanosheets Revealed by Electrochemical and Photoelectrochemical Studies." *j. am. chem. soc.* 126, 2004: 5851-5858.

- [8] Shu-Yen Liu, J. K. Sheu, Chun-Kai Tseng, Jhao-Cheng Ye, K. H. Chang, M. L. Lee, and W. C. Lai. "Improved Hydrogen Gas Generation Rate of n-GaN Photoelectrode with SiO₂ Protection layer on the Ohmic Contacts from the electrolyte." *Journal of The Electrochemical Society*, 2010: B266-B268.
- [9] T. Bak, J. Nowotny, M. Rekas, C.C. Sorrell. "Photo-electrochemical hydrogen generation from water using solar energy. Materials-related aspects." *International Journal of Hydrogen Energy* 27, 2002: 991-1022.
- [10] Todd G. Deutsch, Carl A. Koval, and John A. Turner. "III-V Nitride Epilayers for Photoelectrochemical Water Splitting: GaPN and GaAsPN." *J. Phys. Chem. B*, 110, 2006: 25297-25307.
- [11] Lionel. Vayssieres, *On Solar Hydrogen & Nanotechnology*. Singapore: John Wiley & Sons (Asia) Pte Ltd, 2009: pp.3-32.

Chapter 2 : Basic Principle of Solar Water Splitting

2.1 Introduction of solar water splitting

Solar water splitting is a method to generate hydrogen from water by consuming solar energy collected at the semiconductor alloy as a photo-anode or a photo-cathode. In order to initiate decomposition of water, 1.23eV is the minimum required energy, although practically much higher energy is required due to overpotentials. Basically, a cell for solar water splitting must consist of at least three components: a working electrode made of a semiconductor material, the counter electrode made of metal or another kind of semiconductor material, and an electrolyte. However, for an experimental set up, additional components are required to investigate reactions taking place at only the working electrode; specifically, a reference electrode and a potentiostat are needed. Detailed functions of all components will be explained in chapter 3.1. Since photoelectrochemical reactions take place in the cell, this cell is referred to as a photoelectrochemical (PEC) cell.

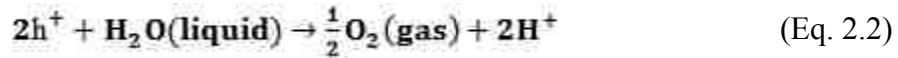
By employing an n-type semiconductor as the working electrode for the PEC cell, the electrode works as a photo-anode upon illumination. An oxidation reaction occurs while hydrogen forms at the counter electrode. When a p-type semiconductor employed as the working electrode, the electrode works as a photo-cathode that hydrogen is evolved under illumination and oxidation reaction takes place at the counter electrode. The details are described in reference 2. This difference in reaction between electrode materials can be explained by the band structure which will be explained in the section 2.3.

2.2 Chemical reaction mechanism in the cell

The chemical reaction of water splitting and threshold energy to induce splitting water will be explained in this section. When an n-type semiconductor is employed for the working electrode in the PEC cell, the electron-hole pair is generated at the working electrode. The reaction is expressed in the following equation:



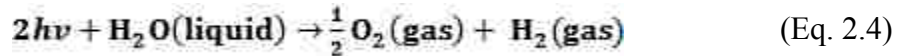
where h is Planck's constant, ν is the frequency, e^{-} indicates the electron, and h^{+} indicates the hole. When the energy of the light, $h\nu$, is equal to or greater than the band gap energy of the material, electron-hole pairs are generated. Water is decomposed into oxygen and hydrogen ions by the generated holes at the electrode. This reaction can be expressed as follow:



where H^{+} indicates the hydrogen ion. While the generation of oxygen occurs at the photoanode, the reduction reaction takes place at the counter electrode where hydrogen ions are reduced into hydrogen gas. This reaction is described by:



Therefore, all reactions can be expressed in one equation, which is shown as follow:



To initiate the reaction of (Eq. 2.4), the reaction energy ($E_{Incident} = h\nu$) is required, which is expressed in this equation:

$$E_{Incidence} = \frac{\Delta G_{\text{H}_2\text{O}}^0}{2N_A} \quad (\text{Eq. 2.5})$$

where $\Delta G_{(\text{H}_2\text{O})}^0$ is the standard Gibbs energy =237.2 kJ/mol at 25 °C and 1 bar and N_A is Avogadro's number = 6.022×10^{23} . Therefore, the threshold energy to initiate water splitting is:

$$E_{\text{Incidence}} = h\nu = 1.23\text{eV} \quad (\text{Eq. 2.6})$$

In other words, the voltage 1.23V across the working electrode and the counter electrode is at the minimum required voltage for decomposition of water.

In our PEC cell, hydrochloric acid is employed as the electrolyte, its half reaction is shown by this equation:



Consequently, there is a possibility that this reaction occurs rather than oxygen generation as described in (Eq. 2.4). Also, decomposition of n-GaN alloy can take place since our experimental result showed that there was some degradation in the n-GaN alloy after two hours of voltage-biased operation under illumination. This decomposition process can be expressed by this equation:



These reactions compete against each other and photo generated electron-hole pairs can react with any redox systems in the PEC cell. There are several factors affecting which reaction can take place, such as the band edge positions, the band gap energy of the semiconductor, as well as the redox potentials and speed of the reactions. The details are described in reference 1, 3, 9, 10 and 11.

2.3 Band structure

In an attempt to obtain an efficient hydrogen generation rate by solar water decomposition, the semiconductor material for the working electrode should satisfy several requirements in order to construct an appropriate band structure in the PEC cell: an appropriate band gap, proper band edge positions, and small overpotentials.

When an n- or p- type semiconductor is illuminated, the Fermi level splits into two quasi-Fermi levels: one is the quasi-Fermi level of electrons E_{nF} , the other one is the quasi-Fermi level of holes E_{pF} , as shown in Figure 2.1.

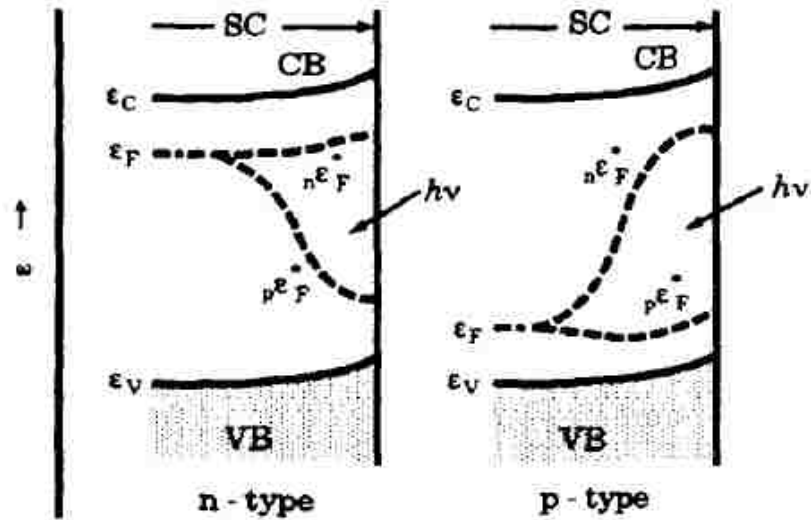


Figure 2.1. The Fermi level splitting into quasi-Fermi levels by photo excitation. The incident light comes from right hand side of this picture. ϵ_f : Fermi level, ϵ_c : Conduction band edge potential, ϵ_v : Valence band edge potential, $p\epsilon_f$: the quasi Fermi level of holes, $n\epsilon_f$: the quasi Fermi level of electrons [7].

If an n-type semiconductor and an electrolyte are brought together, upward band bending is induced in the semiconductor, which is referred to as the depletion layer. Since the Fermi level of n-type semiconductor is generally higher than the redox center, which

is middle of $E_{F(O_2/H_2O)}$ and $E_{F(H^+/H_2)}$. $E_{F(O_2/H_2O)}$ is the redox potential of oxidation reaction and $E_{F(H^+/H_2)}$ is the redox potential of reduction reaction and $E_{F(H^+/H_2)} - E_{F(O_2/H_2O)} = 1.23V$ which is the minimum potential to decompose water into hydrogen and oxygen explained in section 2.2. Then, charging current is induced and the current continuous to flow until thermal equilibrium is achieved. After thermal equilibrium is achieved, there is no net current; any redox reactions cannot come about without photo excitation or applying bias voltage as shown in Figure 2.2.

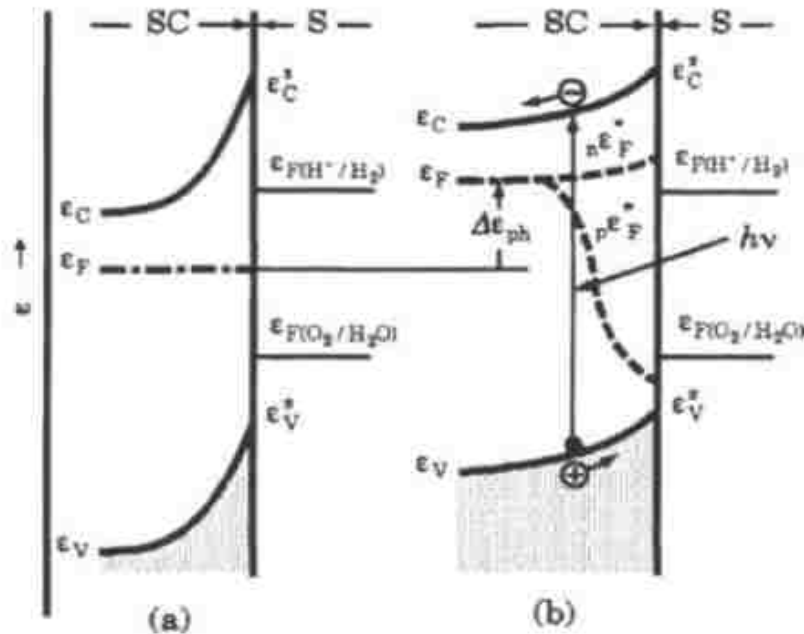


Figure 2.2. (a) The band structure when n-type semiconductor and water are brought together. (b) The band structure under illumination. ϵ_f : Fermi level, ϵ_c : Conduction band edge potential, ϵ_v : Valence band edge potential, $p\epsilon_f$: the quasi Fermi level of holes, $n\epsilon_f$: the quasi Fermi level of electrons [7].

If the reaction potentials of $E_{F(H^+/H_2)}$ and $E_{F(O_2/H_2O)}$ are placed inside of the quasi-Fermi levels of the semiconductor, this semiconductor has a potential to conduct solar water splitting without an applied bias voltage. Therefore, in order to decompose water

without an applied bias, the conduction band edge and the valence band edge of a semiconductor material at the least straddle the reaction potentials of water. K. Fujii *et al.* reported on the band edge positions of GaN, InGaN and AlGaIn relating to redox potentials of $E_{F(H^+/H_2)}$ and $E_{F(O_2/H_2O)}$ [6]. His reports stated that band edge positions of the materials are straddling $E_{F(H^+/H_2)}$ and $E_{F(O_2/H_2O)}$; the potential of the conduction band is higher than $E_{F(H^+/H_2)}$ and the potential of the valence band is lower than $E_{F(O_2/H_2O)}$. Hence, solar water splitting without an applied bias is conceivable with GaN, InGaN or AlGaIn alloy unless the overpotential is large. Figure 1.3, Figure 2.3, and Figure 2.4 show the band edge positions of GaN, InGaN, AlGaIn. Figure 2.5 shows band edges positions of various semiconductors. From these results, there are a few semiconductors can meet this criterion of band edge position, and as a result, GaN, InGaN and AlGaIn are ideal materials in terms of band edge positions for solar water splitting.

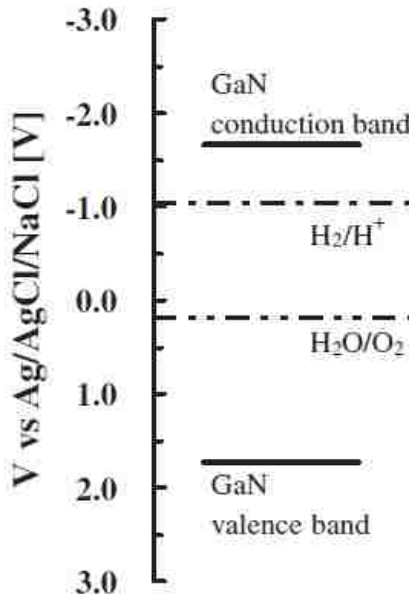


Figure 2.3. Band edge positions of GaN in aqueous 1 mol/L KOH electrolyte (PH = 14). The conduction band edge is higher than the reaction potential of hydrogen and the valence band is lower than the reaction potential of oxygen [6].

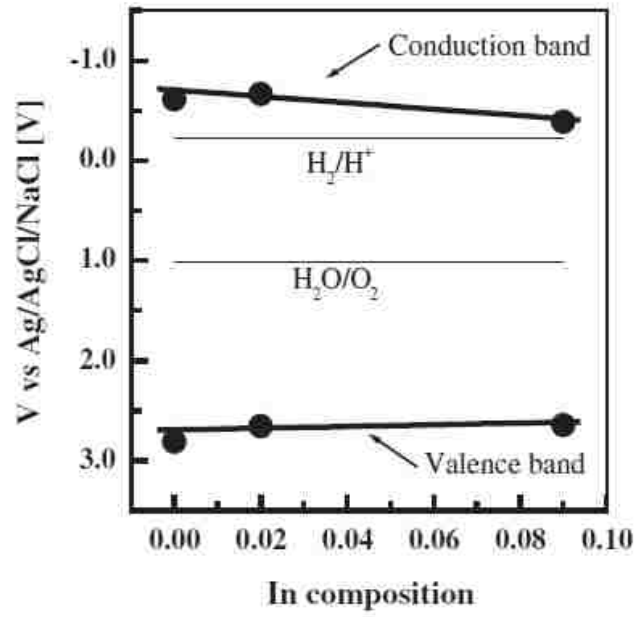


Figure 2.4. Band edge positions of InGaN as a function of In-content in aqueous 1 mol/L HCl electrolyte (pH = 0.1) [6].

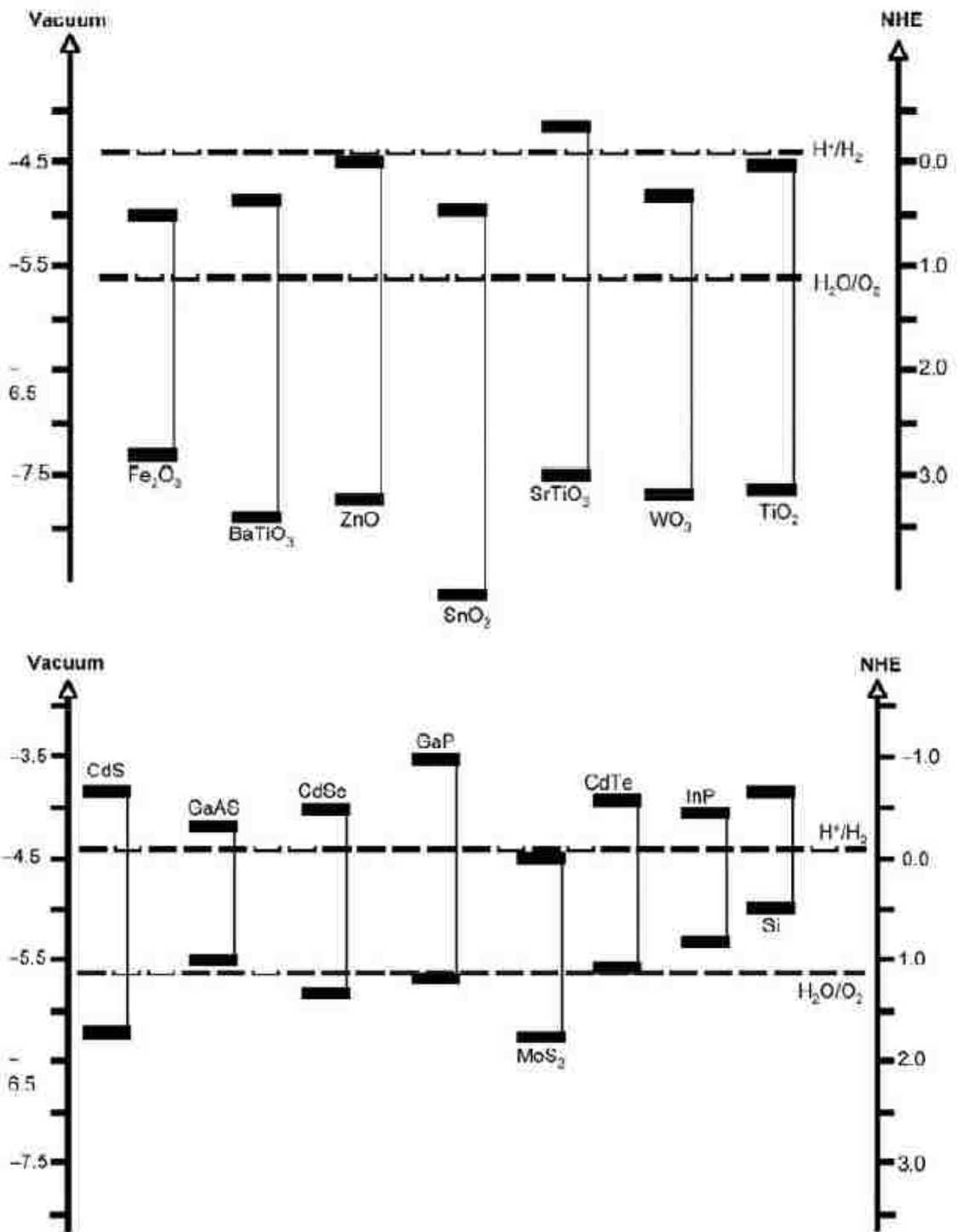


Figure 2.5. Band edge positions of various semiconductors in contact with a pH 1 aqueous solution [2].

Although the energy of 1.23eV is a minimum requirement for decomposition of water, much higher energy is required in order to initiate hydrogen generation in actual PEC cell since there are potential drops other than decomposition of water referred to as overpotentials. In the case of actual PEC cell, the operation voltage can be expressed in the following equation:

$$V_{op} = V_{H_2O} + \eta_a + |\eta_c| + \eta_{\Omega} \quad (\text{Eq. 2.9})$$

where η_a and η_c are the anodic and cathodic overpotentials, and η_{Ω} is the Ohmic overpotential caused by resistive loss in the cell. η_a and η_c are caused by slow reactions of decomposition of water, and large resistivity in the cell results in high overpotentials. In order to increase photocurrent with low or without an applied bias, the overpotentials should be decreased.

Figure 2.6 represents an actual PEC cell that consists of the n-type semiconductor working electrode, the metal counter electrode, and the electrolyte with assumptions. It is assumed that the quasi-Fermi levels are straddling the redox potentials of water, the Fermi level of the metal electrode is lower than the Fermi level of the semiconductor, and the overpotentials are small. In Figure 2.6, (a) represents the open circuit of the PEC cell; there are no contact between them, (b) represents the closed circuit of the PEC cell in the dark; the Fermi levels and the potential of the redox center are equilibrate. Without an applied bias, there is no reaction taking place. Figure 2.6(c) represents the closed circuit under illumination; the quasi-Fermi levels of the semiconductor are straddling both redox potentials of water and the overpotentials. As a result, redox reactions can take place. The details are described in reference 7.

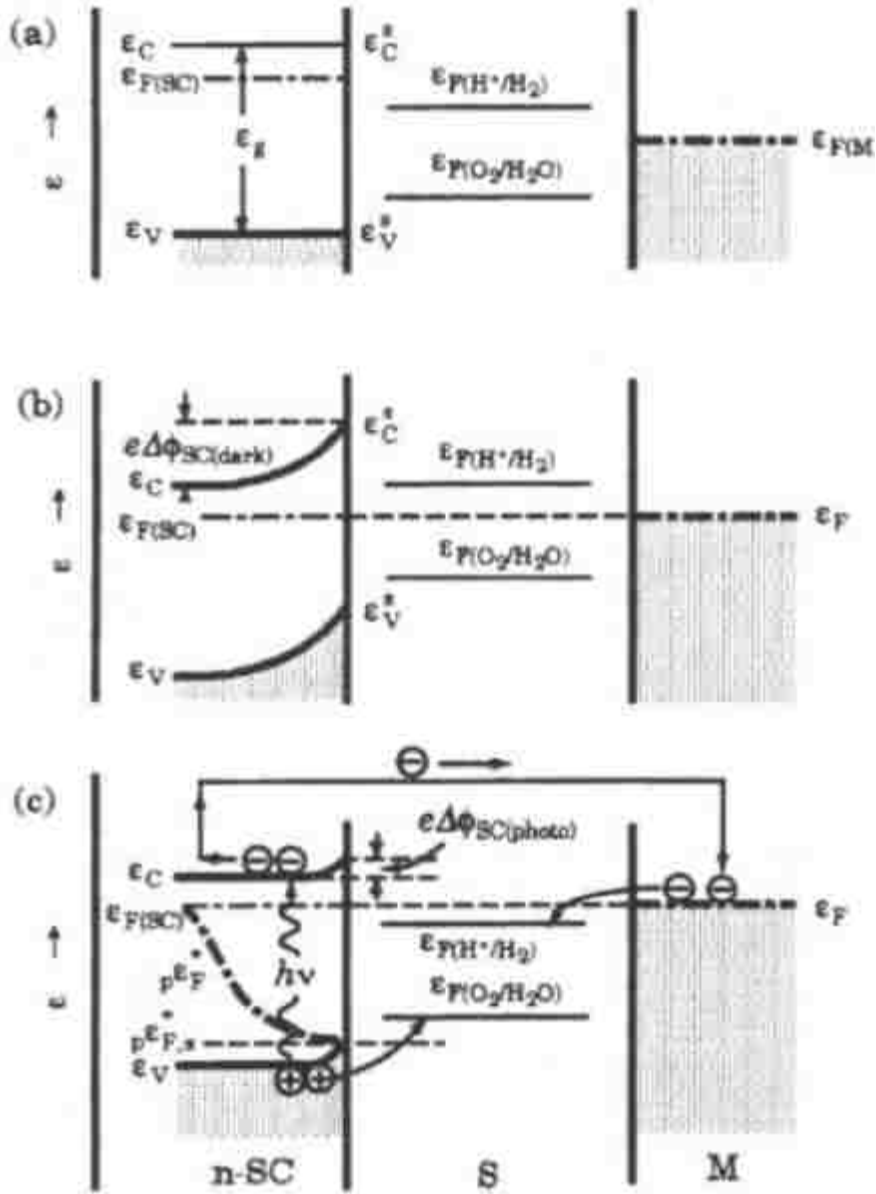


Figure 2.6. Energy diagrams of a PEC cell to decompose water. From left of each picture, n-SC represents an n-type semiconductor, S represents an aqueous solution, M represent a metal electrode. (a) The cell circuit is open. (b) The cell circuit is closed in the dark. (c) The cell circuit is closed under illumination [7].

In conclusion, the semiconductor material for the working electrode should satisfy three conditions in order to decompose water without an applied bias. Firstly, the quasi-Fermi levels must straddle the redox potentials. Secondly, band gap energy of the

material must be larger than sum of 1.23eV and the over potentials, and thirdly, the overpotentials must be small.

2.4 Decomposition of semiconductor

In the previous sections, chemical reactions and band structure are explained. In this section, decomposition of a semiconductor will be explained. Decomposition of the semiconductor by electrolysis can occur through both anodic and cathodic operation. This decomposition process can be formulated as redox reactions in the following equations:



where AB denotes a compound semiconductor, ΔG_a is the free energy change at the photo anode, ΔG_c is the free energy change at the photo cathode, and n is the number of electrons or holes. The free energy changes ΔG_a and ΔG_c can be expressed by enthalpy terms at the anode and cathode in the following equations:

$$E_{p,d} = \frac{\Delta G_a}{nN_A} \quad (\text{Eq. 2.12})$$

$$E_{n,d} = \frac{\Delta G_c}{nN_A} \quad (\text{Eq. 2.13})$$

where $E_{p,d}$ and $E_{n,d}$ are the free enthalpy of oxidation reaction per one hole and of reduction reaction per one electron, respectively. In other words, $E_{p,d}$ is the potential of oxidation reaction of the semiconductor, and the parameter $E_{n,d}$ is the potential of reduction reaction of the semiconductor. Therefore, the decomposition reaction occurs if one of the following conditions is satisfied:

$$E_{pF} < E_{p,d} \quad (\text{Eq. 2.14})$$

$$E_{nF} > E_{n,d} \quad (\text{Eq. 2.15})$$

Even if one of the conditions is satisfied, the material still can be stable when the following conditions are satisfied:

$$E_F(O_2/H_2O) < E_{p,d} \quad (\text{Eq. 2.16})$$

$$E_F(H^+/H_2) > E_{n,d} \quad (\text{Eq. 2.17})$$

Figure 2.5 shows decomposition energy levels of various semiconductors calculated from half reactions and thermodynamic data by Gerischer [5]. These energy levels may vary depending on the final products of the chemical reactions and the electrolyte composition, particularly, ions or molecules in the solution that react with the components of the semiconductor. The details are described in reference 4 and 5.

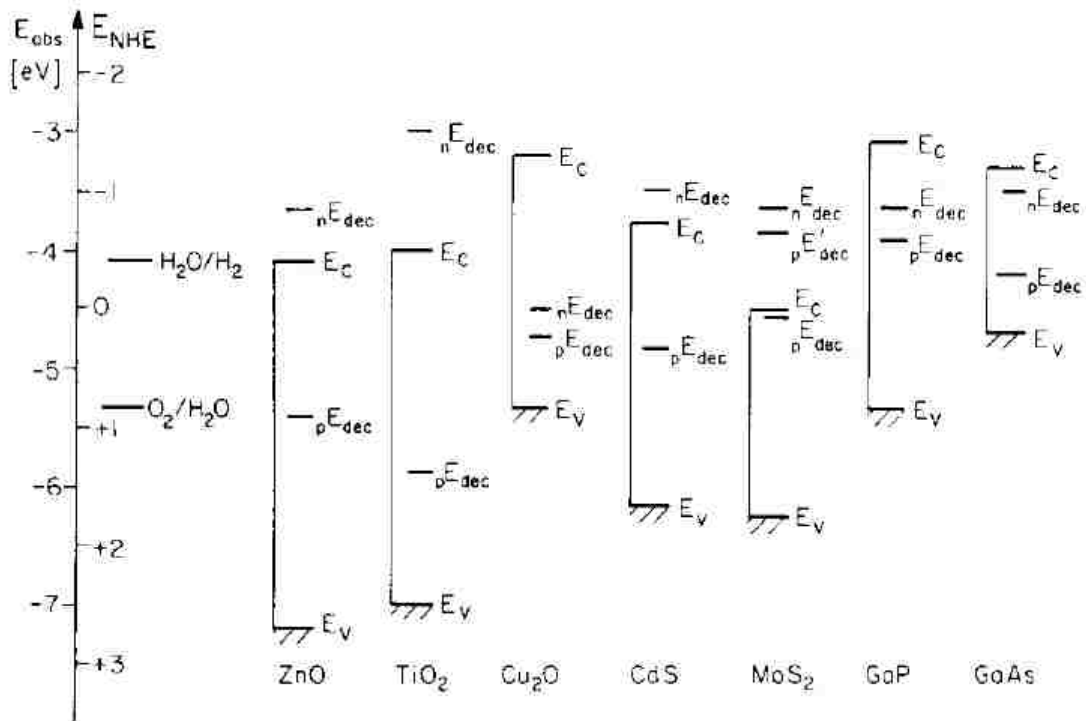


Figure 2.7. Band edge positions and decomposition Fermi energies [4].

According to Gerischer, the decomposition effect of semiconductor in the electrolyte is dependent on the relation of reaction potential positions of all possible reactions [5]. In the case of our PEC cell, reaction potentials of water, oxidation of chloride ions and decomposition potential of GaN or InGaN compete against each other.

2.5 Efficiency of a PEC cell

The efficiency of a PEC cell is defined as the solar conversion efficiency η_c . The solar conversion efficiency η_c can be expressed as:

$$\eta_c = \frac{\text{Energy Stored as hydrogen} - \text{Energy input from power supply}}{\text{Light energy input}} \quad (\text{Eq. 2.18})$$

Thus, the solar conversion efficiency η_c can be calculated by this equation:

$$\eta_c = \frac{\Delta G_{(H_2O),RH_2}^0 - V_{bias}I}{P_t} \quad (\text{Eq. 2.19})$$

where $\Delta G_{(H_2O)}^0$ is the standard Gibbs energy =237.2 kJ/mol at 25 °C and 1 bar, and P_t is the intensity of the illumination (W/m^2). Therefore, the relation can be expressed in the following equation:

$$\eta_c = \frac{(1.23 - V_{bias})I}{P_t} \quad (\text{Eq. 2.20})$$

The expression above represents the fuel cell efficiency, and the details are described in references 2 and 8.

To summarize this chapter, the band structure and the chemical reactions in the PEC cell including decomposition of the semiconductor have been reviewed. In order to decompose water, electron / hole energy of 1.23eV is thermodynamically required as the lower limit of the energy; however, a much higher energy is required in an actual

situation due to the overpotentials. The decomposition of a semiconductor arises when one of the decomposition energy edges are placed between the quasi-Fermi levels of the semiconductor and are placed outside of the redox potentials of water.

Reference for chapter 2

- [1] C. Youtsey, I. Adesida, G. Bulman,. "Highly anisotropic photoenhanced wet etching of n-type GaN." *Appl. Phys. Lett.*, Vol. 71, No. 15, 1997: 2151-2153.
- [2] Craig A. Grimes, Oomman K. Varghese and Sudhir Ranjan. *Light, Water, Hydrogen: The Solar Generation of Hydrogen by Water Photoelectrolysis*. NewYork : Springer Science+Business Media, LLC, 2008: pp.157-179.
- [3] D. Zhuang, J.H. Edgar. "Wet etching of GaN, AlN and SiC." *Material science and Engineering R* 48, 2005: 1-46.
- [4] H. Gerischer "Electrolytic decomposition and photodecomposition of compound semiconductors in contact with electrolytes." *J. Vac. Sci. Technol.* 15(4), 1979: 1422-1428.
- [5] H. Gerischer. "On the stability of semiconductor electrodes against photodecomposition." *J. Electroanal. Chem.*, 82, 1977: 133-143.
- [6] Katsushi. Fujii, Takeshi. Karasawa, Kazuhiro. Ohkawa,. "Hydrogen Gas Generation by Splitting Aqueous Water Using n-Type GaN Photoelectrode with Anodic Oxidation." *Japanese Journal of Applied Physics* Vol.44, No.18, 2005: L543-L545.
- [7] N, Sato. *Electrochemistry at Metal and Semiconductor Electrodes*. Amsterdam: Elsevier Science B. V., 1998: pp.325-371.

- [8] Bruce Parkinson "On the Efficiency and Stability of Photoelectrochemical Devices."
Acc. Chem. Res. 17, 1984: 431-437.
- [9] R.Faulkner, Allen J. Bard and Larry. *Electrochemical Methods - Fundamental and applications 2nd edition.* wiley, 2001: pp.2-19, pp.44.
- [10] T. Bak, J. Nowotny, M. Rekas, C.C. Sorrell. "Photo-electrochemical hydrogen generation from water using solar energy. Materials-related aspects."
International Journal of Hydrogen Energy 27, 2002: 991-1022.
- [11] Lionel. Vayssieres, *On Solar Hydrogen & Nanotechnology.* Singapore: John Wiley & Sons (Asia) Pte Ltd, 2009: pp.3-32.

Chapter 3 : Demonstration of Solar Water Splitting Employing GaN and InGaN Alloy

3.1 Sample Preparation for the working electrode

In this study, all n- and p-type InGaN and GaN thin layers were grown by metal-organic chemical vapor deposition (MOCVD). For the sake of sample growth, trimethylgallium (TMGa), trimethylindium (TMIn) and ammonia (NH₃) were applied as the gallium, indium and nitrogen precursors, respectively. The growth of p-doped InGaN layer was conducted on 2.5µm thick undoped GaN (u-GaN) template grown on c-plane sapphire. The u-GaN template was grown at 1080 °C and buffer u-GaN layer was grown by applying a low growth temperature followed by template growth. The InGaN layer was grown employing TMIn, TEGa and NH₃ as precursors, and N₂ gas was employed as carrier gas. Si doped n-type GaN, Mg doped p-type GaN, and u-GaN (unintentionally doped GaN) were grown on the u-GaN buffer layer. The details are described in reference 2. Hole measurement results for the set of samples employed in this work are summarized in Table 1.

In order to make a metal contact on these semiconductor samples, e-beam evaporation was applied for n-type samples. Ti/Au were deposited on top portion of n-type samples. For p-type samples, Ni was deposited by the e-beam evaporation and Au was deposited by the thermal evaporation. There was no reason why the thermal evaporator was employed instead of the e-beam evaporator other than there was not convenient machine time of the e-beam evaporator. After the metal deposition on p-type samples, the samples were baked at 540 °C under atmosphere to convert the contact into

an Ohmic contact. By following fabrication of the metal contact, a platinum wire was attached on the metal contact on the sample and it was covered and fixed with epoxy resin. Figure 3.1 shows the working electrode after the platinum wire was attached.

Table 1. Electrical properties of n-GaN, u-GaN, p-GaN, and p-InGaN samples employed in this work.

Sample	Mobility [cm ² /V·s]	Carrier Concentration [cm ⁻³]	Resistivity [Ω·cm]
n-GaN 1	245	-3.2×10^{18}	0.008
n-GaN 2	223	-3.7×10^{18}	0.008
n-GaN 3			
u-GaN	260	-1.5×10^{17}	0.161
p-GaN	4	3.1×10^{17}	4.73
p-InGaN 1	6	2.3×10^{18}	0.445
p-InGaN 2	3	6.7×10^{18}	0.285
p-InGaN 3	2	1.5×10^{18}	1.954

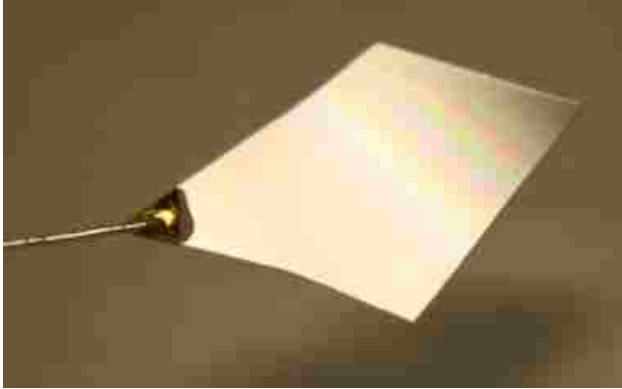


Figure 3.1. The semiconductor working electrode.

3.2 Set up for the experiment

The whole system of our PEC cell is presented in Figure 3.2 and schematic diagram of the PEC cell is shown in Figure 3.3. The PEC cell consists of a potentiostat, a solar simulator and three electrodes: the working electrode, the counter electrode, and the reference electrode, immersed in the electrolyte.

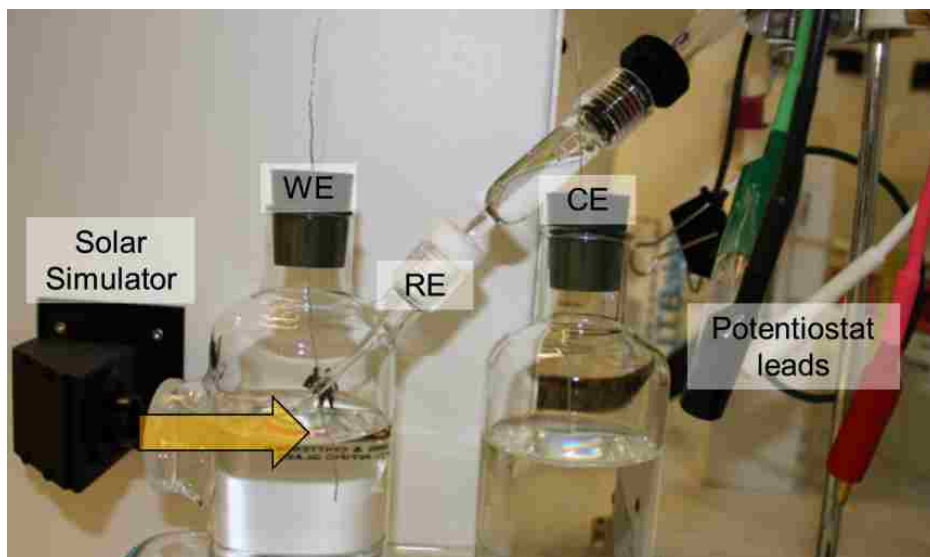


Figure 3.2. The PEC cell. WE: Working electrode. CE: Counter electrode. RE: Reference electrode.

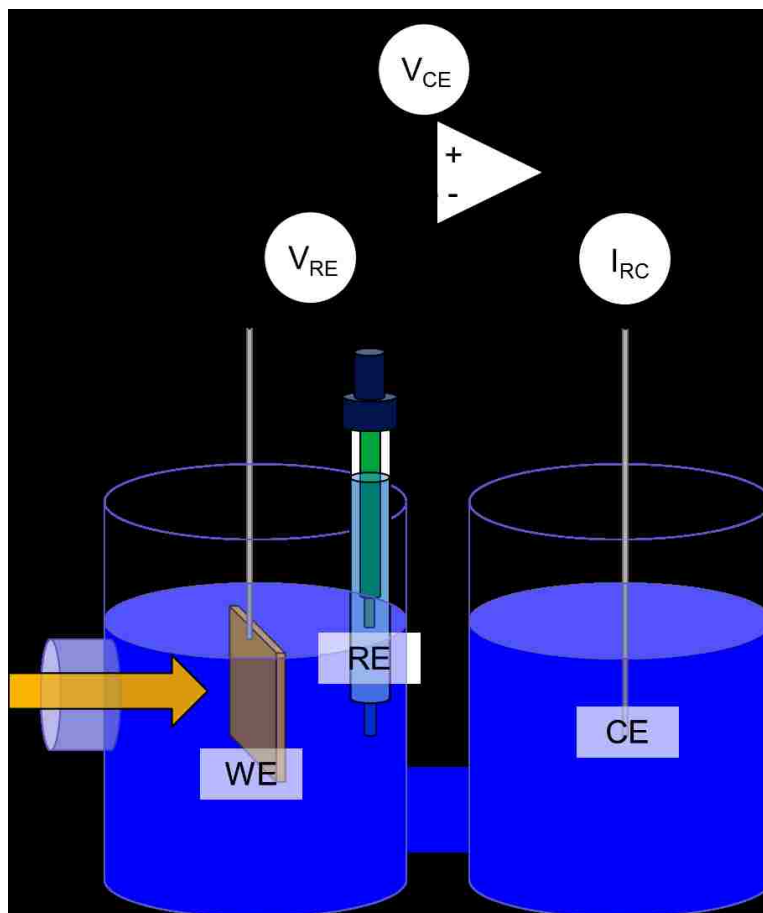


Figure 3.3. Schematic diagram of our PEC cell. Symbols represent as follows: CE: Counter electrode. RE: Reference electrode. WE: Working electrode. I_F is equivalent to reaction-current. "Electrochemical Sensor" denotes the PEC cell and "Vcell" is equivalent to V_{RE} in this thesis.

The detailed explanations regarding components of the PEC cell are listed as followed:

Potentiostat

Potentiostat is electrical device that can control the voltage across the working electrode and the reference electrode by applying current from the counter electrode to the working electrode. Since there is no current flow from or to the reference electrode, there is no double layer constructed around the reference electrode. Therefore, measured voltage is exclusively affected by reactions arising at the working electrode. Figure 3.3 shows basic schematic of a potentiostat. Ezstat (Nuvant) is employed for our PEC cell. The details functions of a potentiostat are described in reference 8

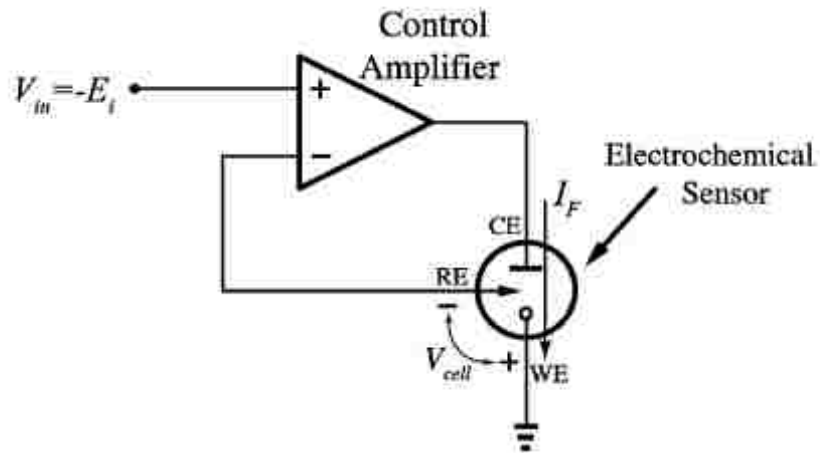


Figure 3.4. Basic schematic diagram of potentiostat [8]. Symbols in this diagram represent as follows: CE: Counter electrode. RE: Reference electrode. WE: Working electrode. I_F is equivalent to reaction-current. “Electrochemical Sensor” denotes the PEC cell and “V_{cell}” is equivalent to V_{RE} in this thesis.

Working electrode and Counter electrode

n- and p- type of GaN alloys, and p-type of InGaN alloys were employed as the working electrode and a platinum wire with 0.3mm in diameter was used as the counter electrode in this experiment. The platinum wire was used because the counter electrode

must be stable in acid for long periods although reactions occurring at this side do not affect reactions occurring at the working electrode side during potentiostatic operation. The detail of the preparation process for the working electrode has been explained in section 3.1.

Reference electrode

A reference electrode is an electrode whose chemical potential with respect to the standard hydrogen electrode (SHE) is known. In this experiment, an Ag/AgCl electrode was employed as the reference electrode. Ag/AgCl is commonly used as reference due to its low price, easy handling, and stable response. The chemical potential of the Ag/AgCl electrode is 0.197eV with respect to SHE. In order to obtain the potential with respect to SHE from measured value, calculation is necessary; $E_{NHE} = E_{Measured} + 0.197 \text{ eV}$.

Solar simulator

The solar simulator of model 10500 (ABET TECHNOLOGIES) is employed for out PEC cell. During the experiment, the solar simulator was placed at a distance from the surface of the semiconductor alloy of the working electrode in order to obtain the intensity of 100 mW/cm^2 at the surface which is equivalent to 1 sun. The beam spot size is 35 mm in diameter.

Electrolyte

A 1 mol/l hydrochloric acid solution is employed as the electrolyte for the PEC cell. pH level was monitored by the pH meter, HM-Digital 200, before the working electrode was immersed into the electrolyte. During this experiment, the pH level was maintained between 0.5 and 0.6.

The working electrode was immersed in the electrolyte except the region of the metal contact on the semiconductor alloy and the platinum wire connected to a working lead from the potentiostat. In order to conduct voltammetry, a recipe to control the voltage across the working electrode and the reference electrode was designed as shown in Figure 3.5 and Figure 3.6. During positive voltage operation, the working electrode works as an anode and oxidation reaction takes place. During negative voltage operation, the working electrode works as a cathode and reduction reaction takes place.

3.3 Results of the experiment

Solar water splitting without an applied bias voltage

Solar water splitting without an applied bias voltage was conducted employing n-GaN, u-GaN, p-GaN and p-InGaN for the working electrode, using a platinum wire for the counter electrode immersed into hydrochloric acid (pH = 0.5), and the solar simulator for the illuminator. The result showed that hydrogen generation was observed when n-GaN was employed for the working electrode.

After the solar simulator was turned on, hydrogen generation was visible at the counter electrode within one minute in the PEC cell with the n-GaN working electrode. There were no bubbles arising at the working electrode while the reaction was taking place. It indicated that corrosion took place on the surface of n-GaN alloy. This generation of hydrogen bubbles without an applied bias voltage was reported by M, Ono *et al.* [7]. There were no bubbles observed when u-GaN, p-GaN, or p-InGaN was employed as the working electrode within 5 minutes.

Solar water splitting with an applied bias voltage

After the experiments without an applied bias voltage, bias voltage was applied to assist the solar water splitting and to investigate characteristic of the PEC cell with each semiconductor alloy electrode. In this experiment, two voltage control modes were utilized for bias control to obtain current - voltage curves. One mode was control of the voltage across the reference electrode and the working electrode. This operation provides current - V_{RE} relation. The current represents reaction current which is correspondent to the amount of reactions taking place on one side of the electrodes. The voltage V_{RE} with respect to the reference electrode was directly relating to the interface phenomena since the other half reaction taking place at the counter electrode can be negligible during this operation. This V_{RE} is exclusively depends on reactions taking place at the working electrode. The counter electrode of the platinum wire acted as the current path in this operation mode, therefore, the counter electrode requires a high resistivity toward the electrolyte under a voltage applied condition. The other operation mode is controlling a voltage (V_{CE}) between the counter and the working electrode and provides the current - V_{CE} relation. This current represents reaction current as well. This V_{CE} directly relates to the actual voltage to initiate hydrogen generation reaction with two electrode system. Before the measurements of these voltages were performed on each working electrode sample, a couple of sweeps of voltage with a triangle wave was carried out to stabilize the current.

The n-GaN working electrode

Solar water splitting employing n-GaN alloy as the working electrode was performed. These working electrode samples for this experiment were named n-GaN 1, n-GaN 2, and n-GaN 3. Concerning n-GaN 1, keystone wave was applied to control bias voltage as shown in Figure 3.5. Concerning the other samples of n-GaN 2 and n-GaN 3, triangle wave was applied which bias voltage is shown in Figure 3.6. The n-GaN 2 and n-GaN 3 were identical characteristic since they were divided samples from one identical sample. Sample names with measurement conditions are presented in the legends of the charts; “light” indicates that the working electrode was under illumination and “dark” indicates that the experiment was conducted in the dark condition.

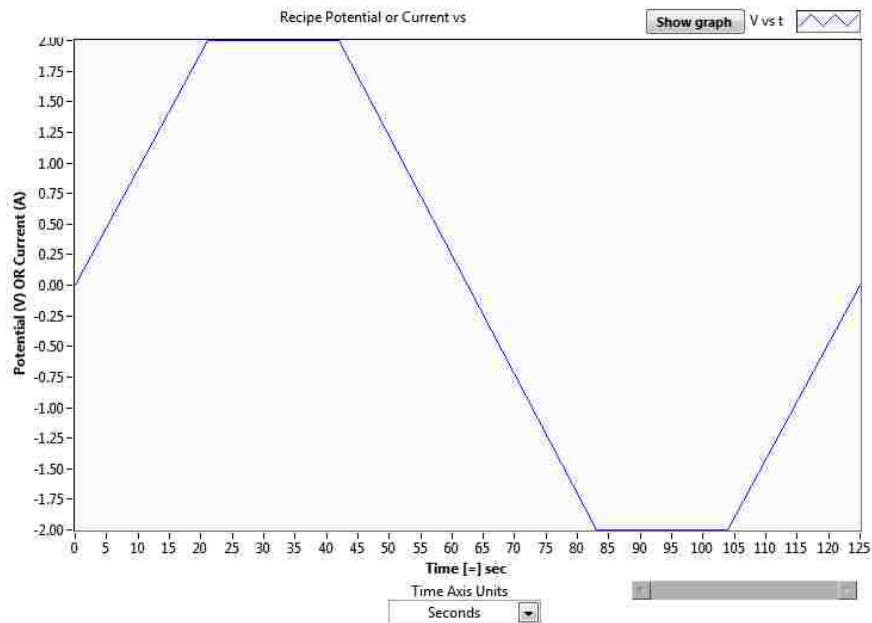


Figure 3.5. Control voltage in keystone shape. When a measurement was conducted in keystone shape, this shape was applied although maximum voltage was modified depending on samples.

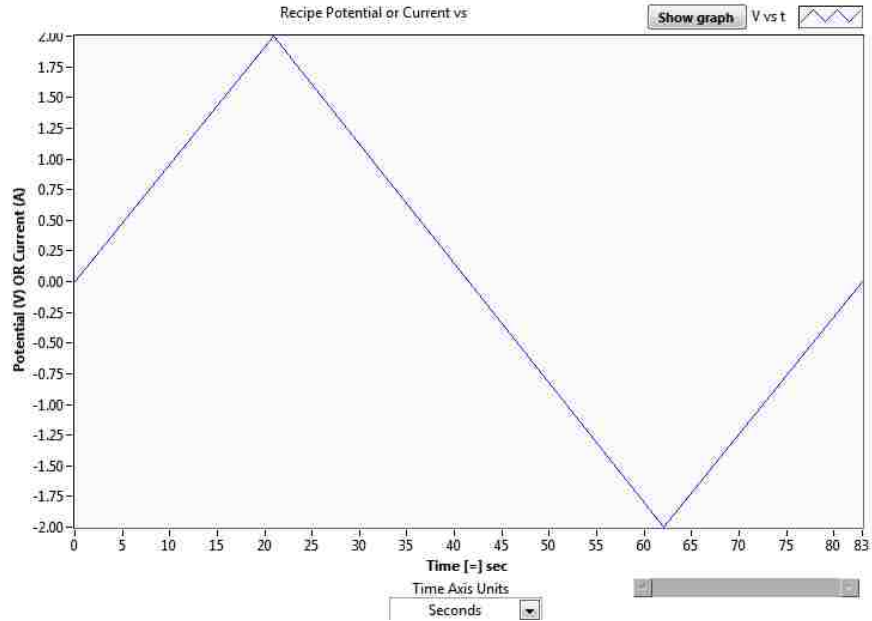


Figure 3.6. Control voltage in triangle shape. When a measurement was conducted in triangle shape, this shape was applied although maximum voltage was modified depending on samples.

Figure 3.7 shows current - V_{CE} relation of the “n-GaN 1” working electrode. Hydrogen generation was visible at the counter electrode when the working electrode was positively biased under illumination. Current density is defined as the whole reaction current divided by the surface area of the semiconductor working electrode in contacting with the electrolyte. Hydrogen bubbles forming at the counter electrode were observed in the PEC cell at each n-GaN working electrode. However, there were no bubbles at the surface of the semiconductor working electrode itself during positive bias operation.

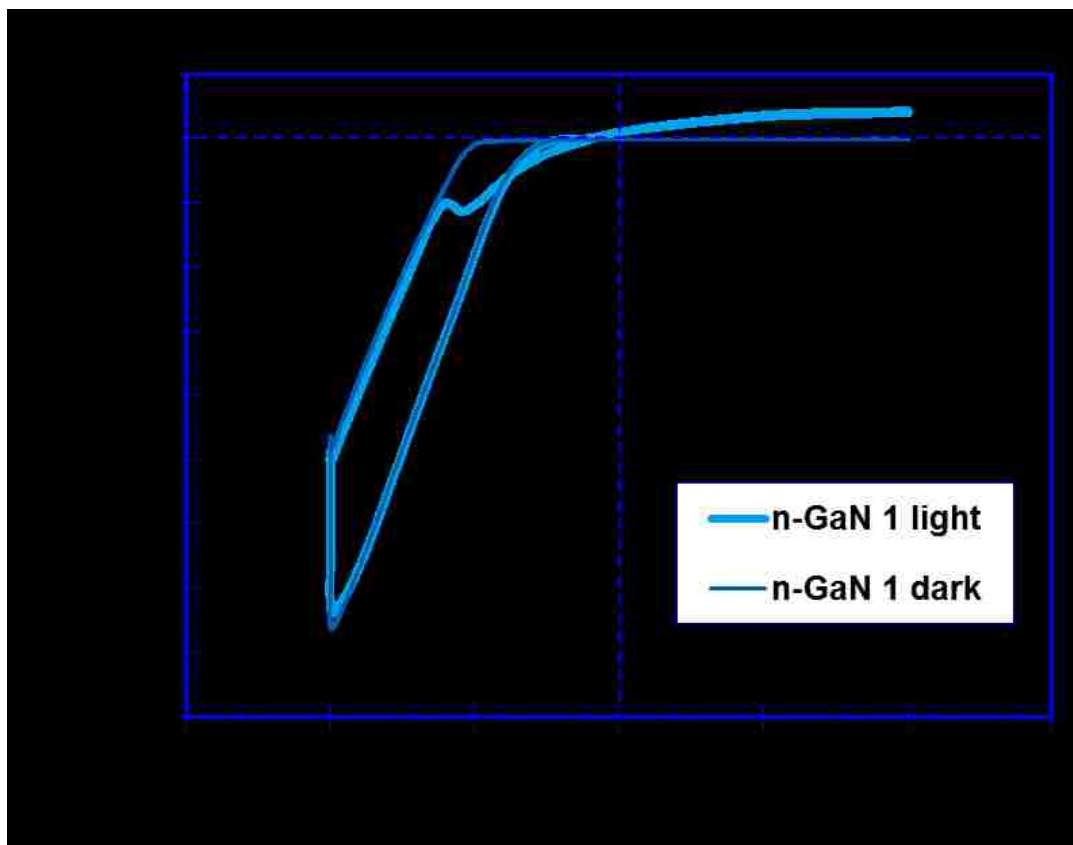


Figure 3.7. Current density – V_{RE} [V vs Ag/AgCl] curve of n-GaN 1.

Figure 3.8 compares the current density – V_{RE} curves of three of n-GaN working electrode samples. It showed comparable reaction toward light illumination by the solar simulator; at positive operation region, the current density was negligible ($\sim 0 \text{ mA/cm}^2$) for three of them in the dark. After the solar simulator was turned on, the photo-current was increased in the equivalent trends between all samples. As explained in chapter 2, the n-GaN alloy works as a photo-anode. It indicates that oxidation reaction should have taken place at this side during positive bias operation. However, any reactions were not visible. Therefore, corrosion occurred at the surface of the n-GaN alloy rather than generation of a gas.

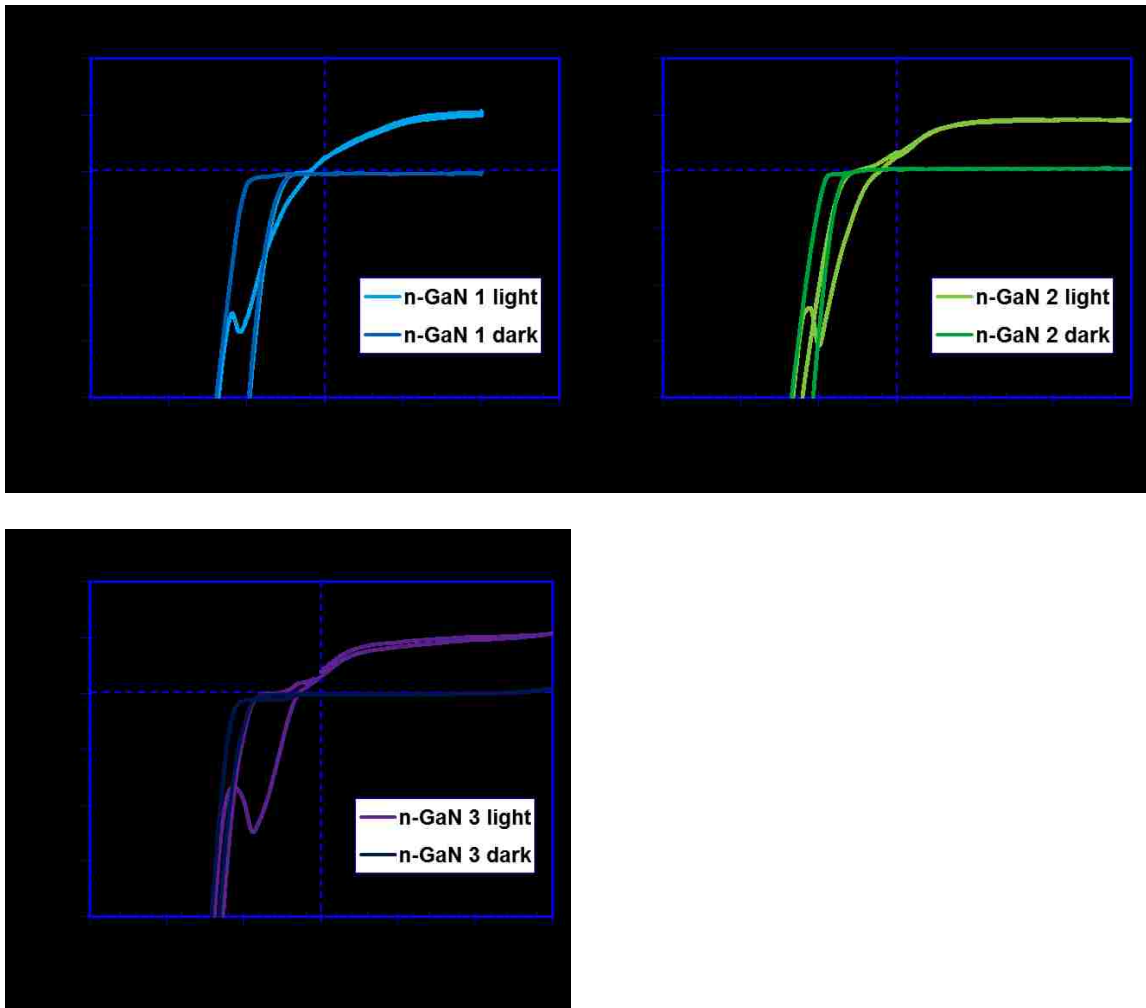


Figure 3.8. Current density – V_{RE} [V vs Ag/AgCl] curves for n-GaN 1, n-GaN 2 and n-GaN 3 under illumination and in the dark are presented.

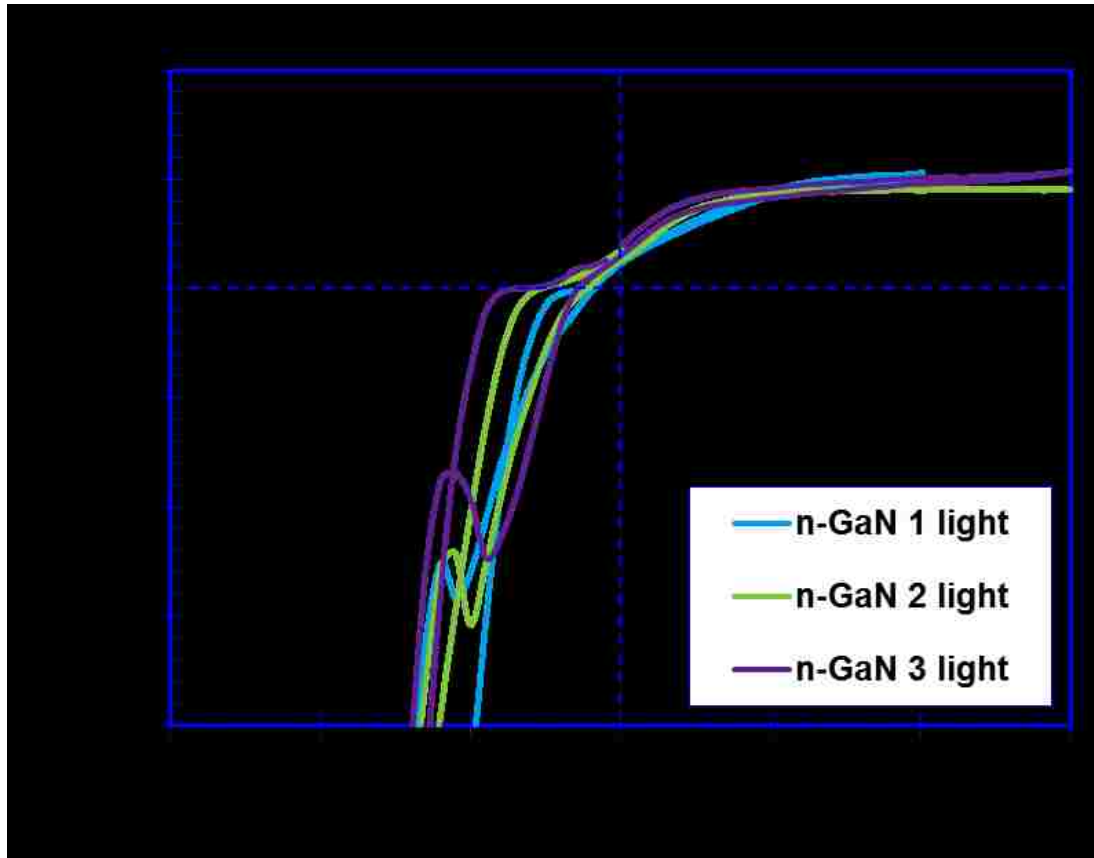


Figure 3.9. Current density - V_{RE} curves of n-GaN 1, n-GaN 2 and n-GaN 3 under illumination.

In Figure 3.10, the result of “nGaN 1 dark” is compared with a result of cyclic voltammetry for n-GaN alloy demonstrated by S. Usui *et al* [9]. There were quite comparable trends between them in positive bias operation. The difference in the cathodic operation regime was due to a difference in sweep range. Our result was obtained by voltage swept from -2V to 2V. In contrast, S. Usui *et al* [9] employed a narrower range, which was from -1V to 1.5V. Thus, in our case, a condenser component in an equivalent circuit for a PEC cell was more charged than that of their experiment and it affected the result. With regard to the equivalent circuit of the PEC cell with the GaN electrode, J. D. Beach *et al.* were reported [3].

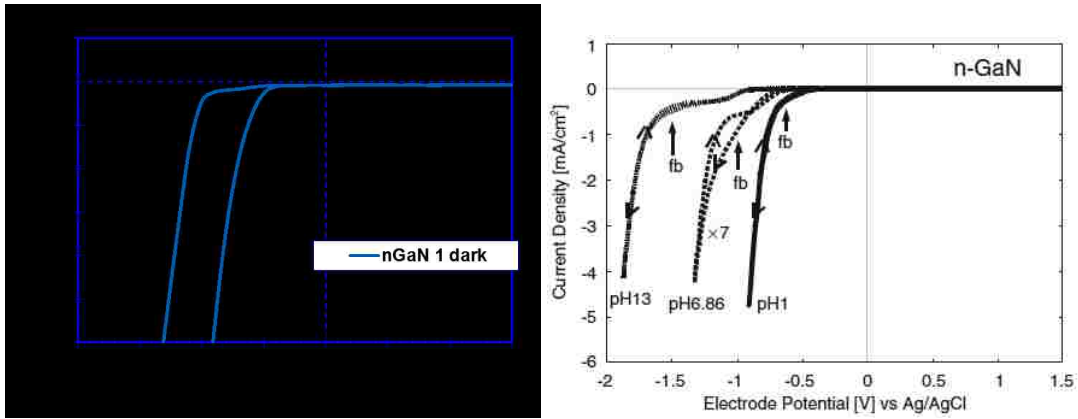


Figure 3.10. Current density - V_{RE} curves. The left chart is from our work. The right chart is reported by S. Usui *et al* [9].

The Figure 3.11 shows current density - V_{CE} curve for “n-GaN 1 light”. There is a hysteresis; the currents were not the same in negative direction sweep and in positive direction sweep owing to the condenser component in the equivalent circuit.

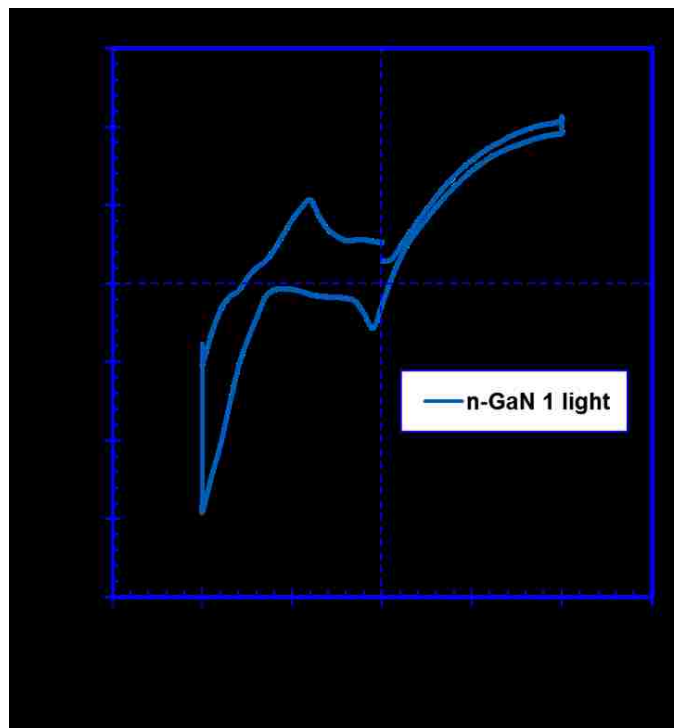


Figure 3.11. Current density as a function of V_{CE} . There is a discontinuity at 0V because the sweep to obtain this result was from 0V to 2V, 2V to -2V and -2V to 0C.

Figure 3.12 shows current density - V_{CE} curves and makes a comparison between our result and that result regarding solar water splitting with n-GaN alloy as the working electrode reported by K. Fujii *et al.* [5]. There was a difference due to the measurement direction.

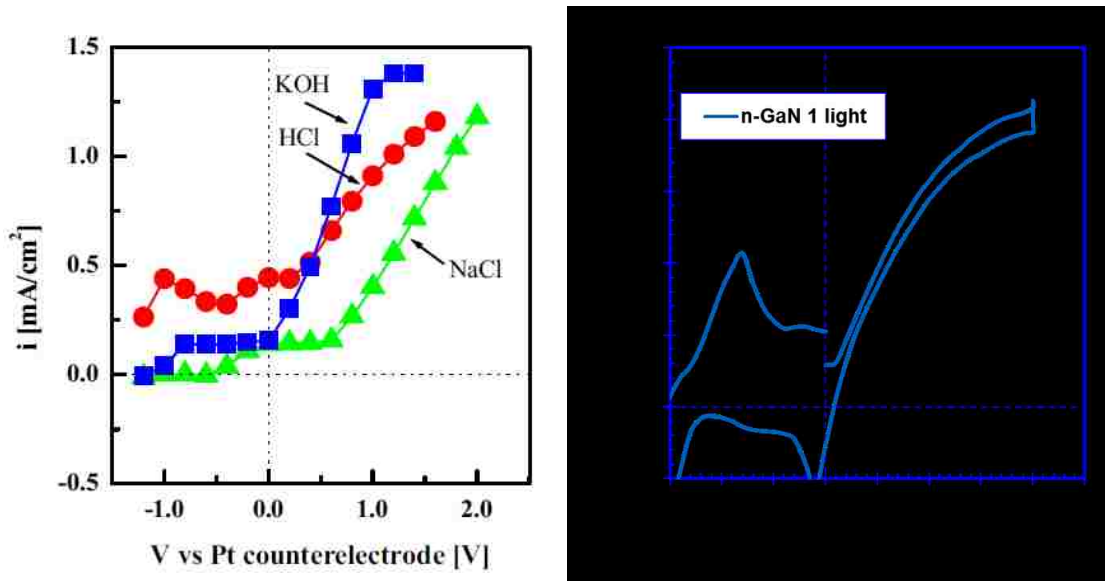


Figure 3.12. Comparison for n-GaN working electrode between the result reported by K. Fujii *et al* and our result which is the same data shown in Figure 3.11. The red curve in the left chart is compatible condition to our result. It shows that our result was reliable [5].

After the experiment run for two hours, color change on the surface of the sample of “n-GaN 1” and photocurrent degradation were observed. Figure 3.13 shows degradation of current density of n-GaN alloy. In this experiment, the solar simulator was kept on and, the V_{CE} was maintained at 2V. There were three peaks in this chart due to the recipe duration. The recipe employed in this experiment maintained the control voltage at 2V for ten minutes, for that reason, every ten minutes the applied bias voltage became 0V and then recovered to 2V. During these switching times, the peaks in reaction currents were observed, which can be attributed to the condenser component in the equivalent

circuit of the PEC cell. The peaks in the reaction current, as shown in figure 3.14, have also been reported by K. Aryal *et al* [4] as an initial current drop for p-GaN and p-InGaN .

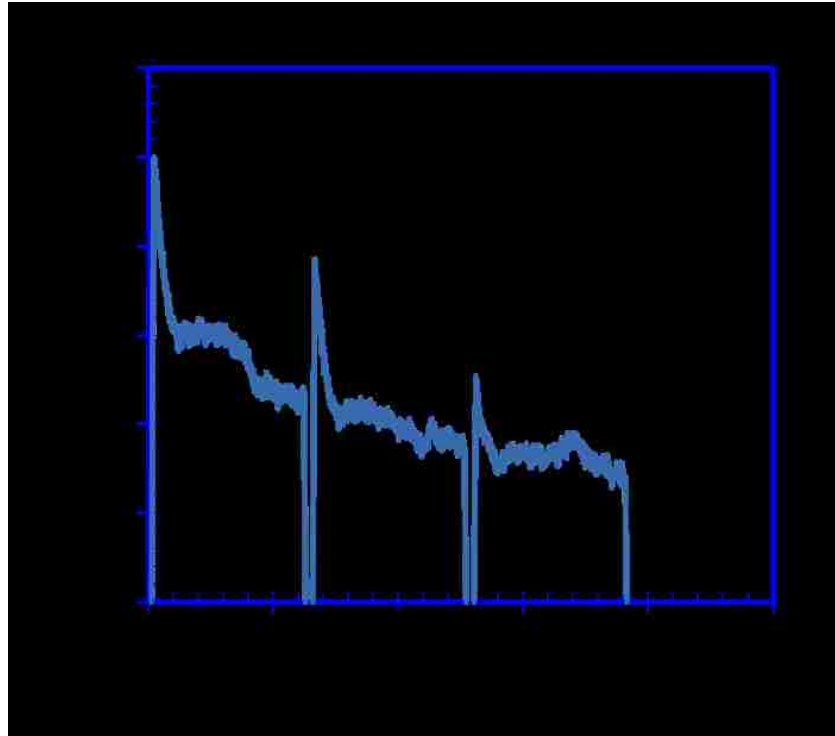


Figure 3.13. Current density of n-GaN 1 as a function of time. There are three peaks due to the switching of the potentiostat; the duration of the recipe applied for this experiment was 10 minutes, accordingly, and peaks arose every 10 minutes.

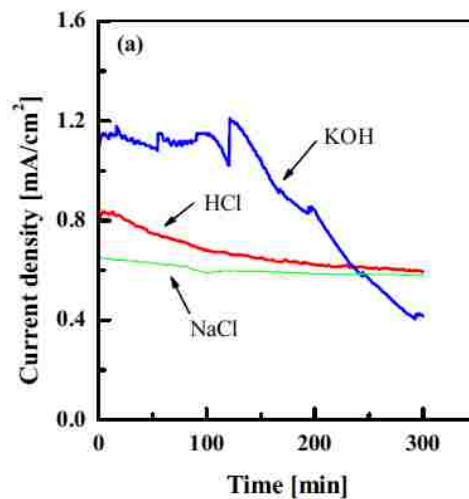


Figure 3.14. Time-dependences of current density of the n-GaN in aqueous 1mol/L HCl solution under illumination. The applied bias across the working electrode and the counter electrode was +1.0V [5].

The u-GaN working electrode

The experiment employing u-GaN as the working electrode was conducted. Keystone shape was applied to control voltage which is shown in Figure 3.5. According to Figure 3.14 and Figure 3.15, the current almost linearly increased as the voltage increased under illumination. Concerning this u-GaN alloy, hydrogen generation was also observed at the counter electrode side, and there was also no visible reaction at the u-GaN surface during positive bias operation. During negative bias operation, bubbles formed at the working electrode and the counter electrode. These reactions at the surface of the u-GaN alloy were comparable to the reactions observed with the n-GaN alloy.

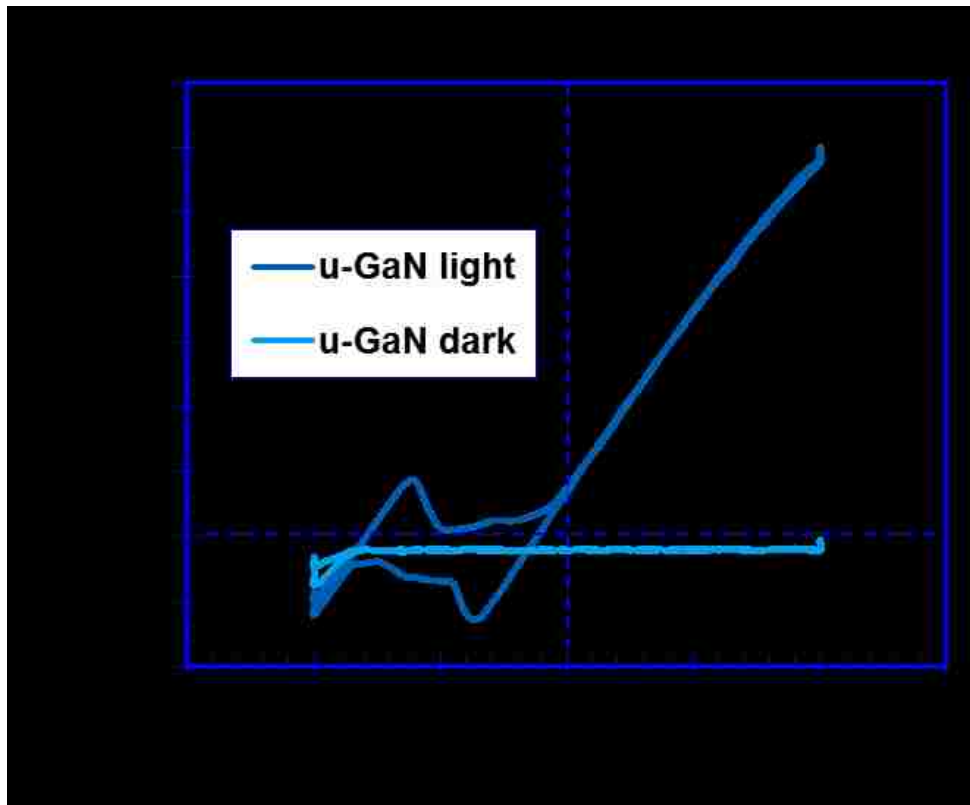


Figure 3.15. Current density as a function of voltage V_{CE} .

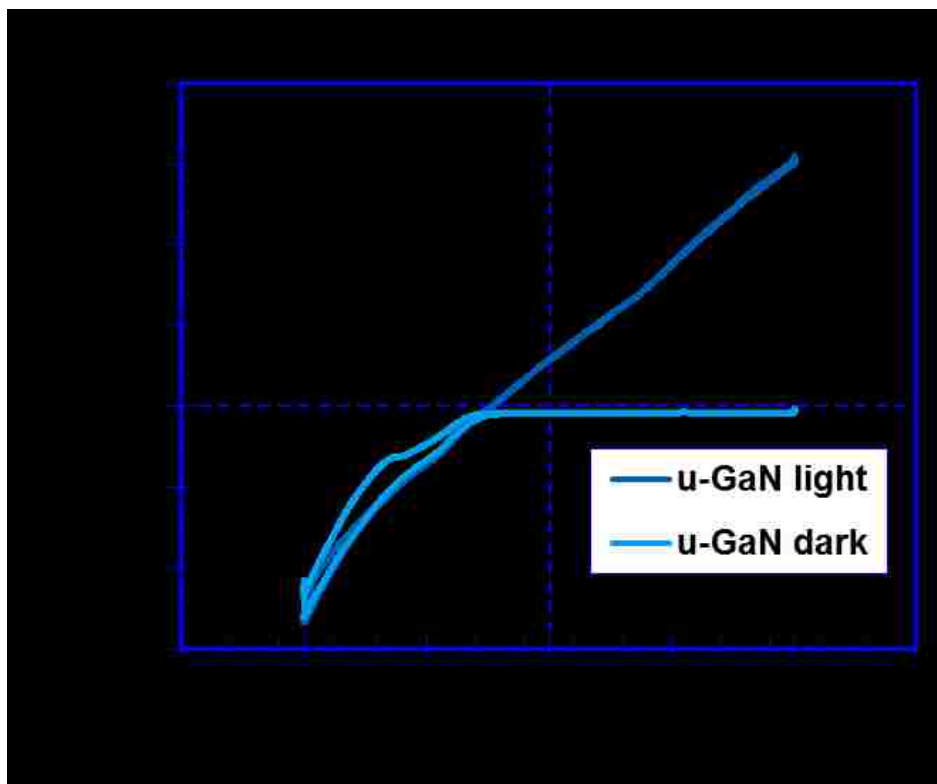


Figure 3.16. Current density as a function of voltage V_{RE} .

The p-GaN and p-InGaN working electrode

Solar water splitting employing a p-GaN alloy or a p-InGaN alloy as the working electrode was also conducted applying the control voltage shown in Figure 3.5. These working electrode samples of p-InGaN alloys were named p-InGaN 1, p-InGaN 2, and p-InGaN 3. The results of current density - voltage curves are shown in Figure 3.17, Figure 3.18, Figure 3.19, and Figure 3.20. These results showed they were comparable trends; the current density under illumination increased much faster than the current density in the dark along with the applied bias voltage increasing for all p-type samples. The observation of the hydrogen bubbles at the working electrode is relatively minimal, due to the extremely low reaction current in this experiment.

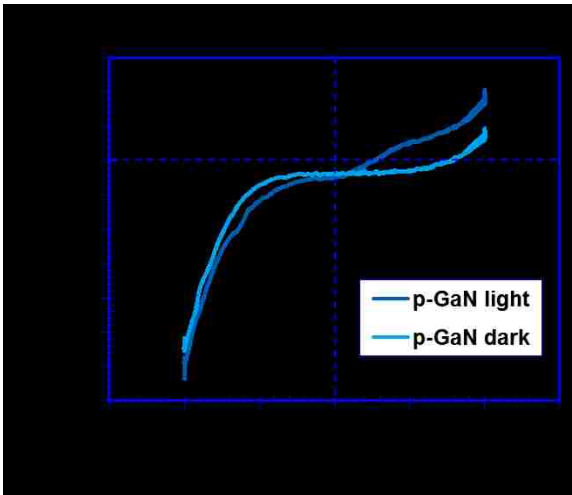


Figure 3.17. Current density – V_{RE} curves for the p-GaN alloy.

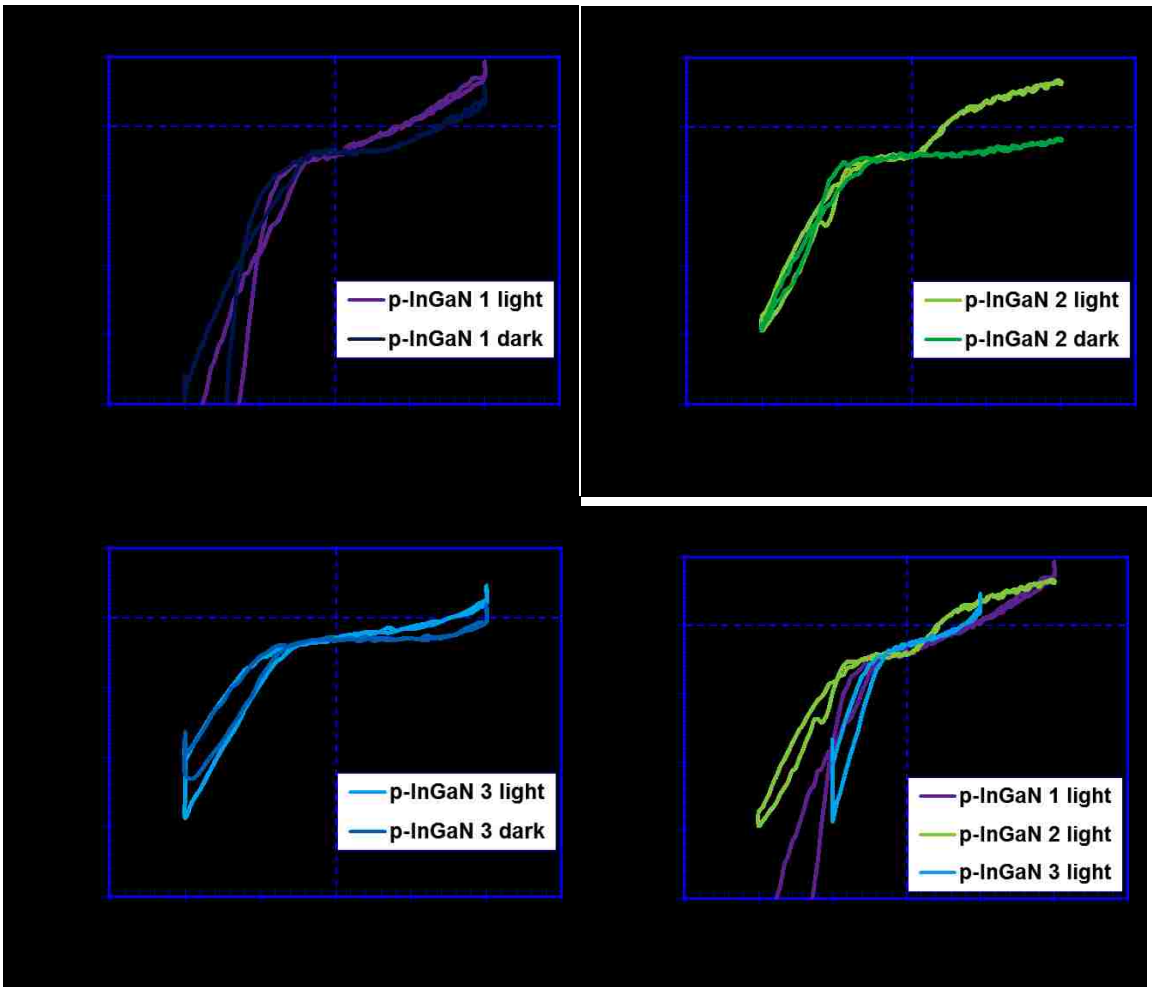


Figure 3.18. Current density as a function of V_{RE} for p-InGaN alloys.

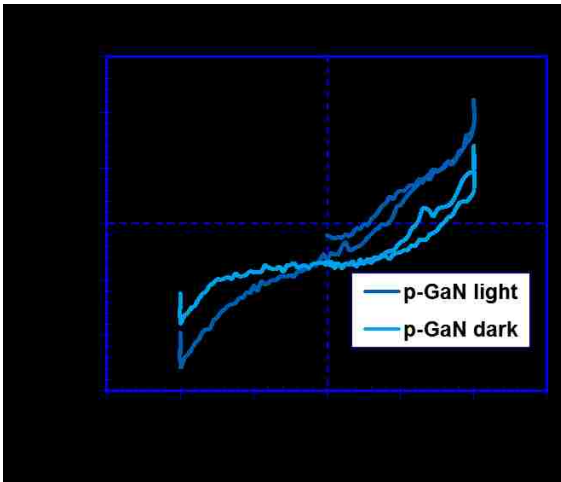


Figure 3.19. Current density – V_{CE} curves for the p-GaN alloy.

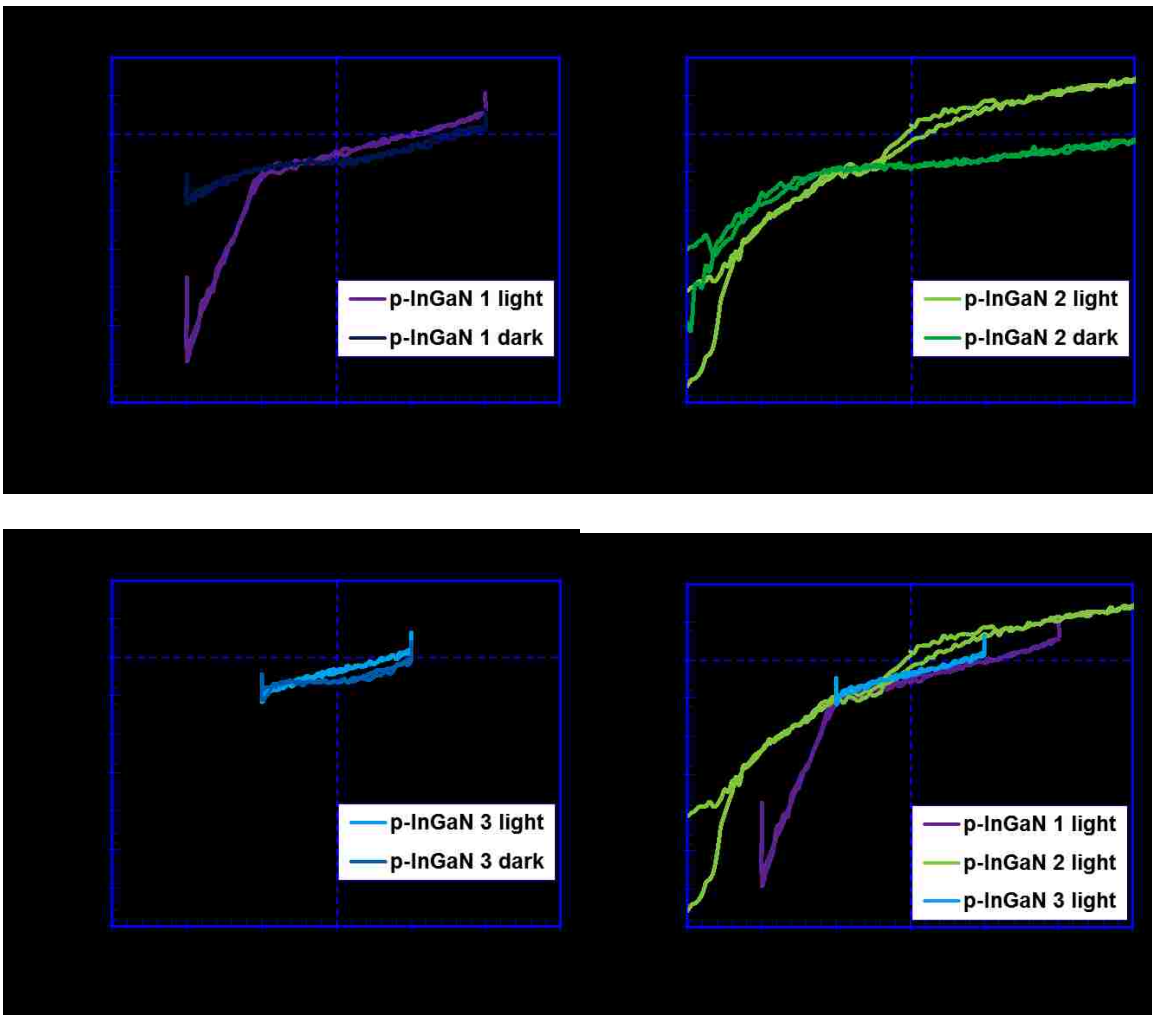


Figure 3.20. Current density – V_{CE} curves for p-InGaN alloys.

Figure 3.21 shows comparison between all semiconductor samples in current - V_{CE} curve. According to this result, the maximum reaction current can be obtained with the n-GaN working electrode in the PEC cell. The difference in reaction currents correspond to a difference in hydrogen generation rate. The difference in reaction current between n-type and p-type GaN semiconductor electrode can be explained by the carrier concentration difference as interpreted by S. Usui *et al* [9].

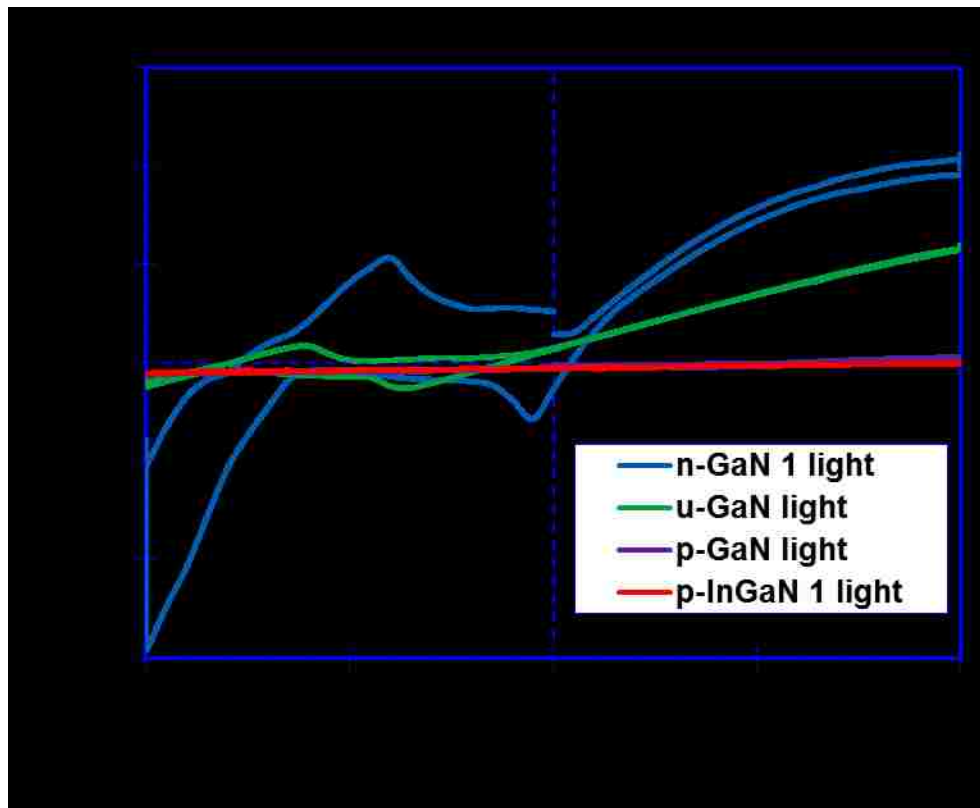


Figure 3.21. Current density as a function of V_{CE} for the sake of comparison in hydrogen generation rate under the same condition of the applied bias voltage and illumination.

Figure 3.22 shows current - V_{CE} curves in reverse order of axes to make a comparison with the results reported by Aryal and co-workers [4]. Both of the results showed

comparable correlations between p-InGaN and p-GaN; both of the results have an onset voltage from which current density for p-InGaN alloy working electrodes increased much quicker than that of the p-GaN alloy working electrode. However, the onset voltages were not equivalent between these two experiments. Our experiments indicated 2.2V onset voltage, while the onset voltage of 0.7 V was reported by Aryal and co-workers [4].

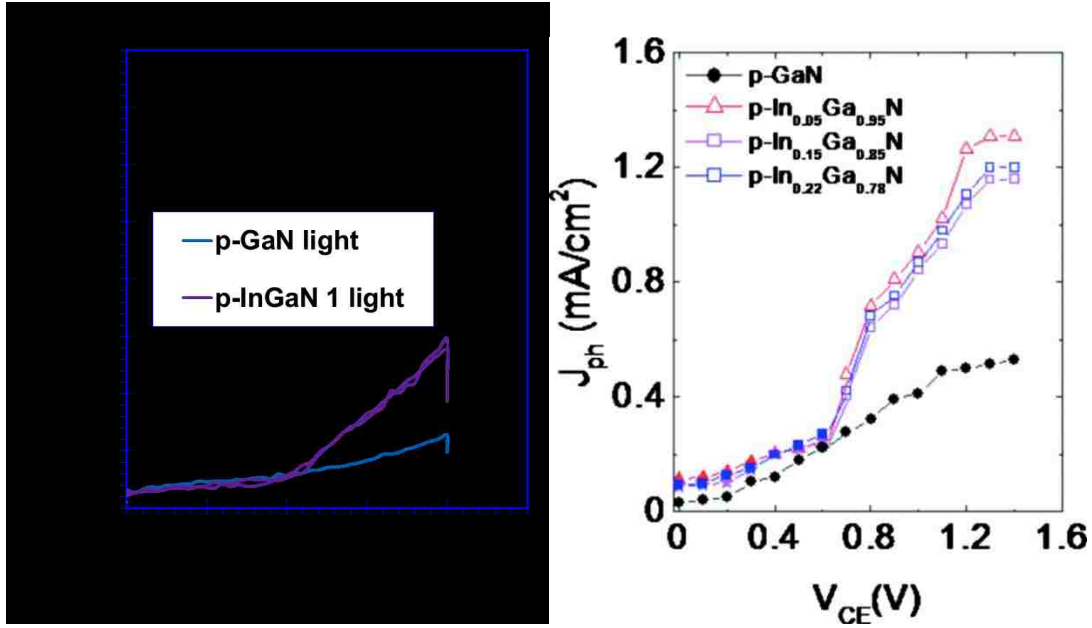


Figure 3.22 Current density - V_{CE} in reverse order of axes. Left is from this work, right is reported by K. Aryal *et al.* [4].

The difference in onset voltage between our work and K. Aryal's work cannot be explained by a difference in the setup. K. Aryal employed hydrobromic acid as the electrolyte which has the half reaction, while hydrochloric acid was employed in our work. The half reaction of hydrobromic acid can be expressed by the following equation:



The standard potential of this half reaction is 1.09eV. By contrast with our case, $2\text{Cl}^- + 2\text{h}^+ \rightarrow \text{Cl}_2$ with standard potential of 1.36eV (Eq. 2.7) was most likely occurred in our PEC cell. This difference in reaction potential appears lesser compared to the difference in onset voltage of hydrogen generation. Previously, S. Usui *et al* [9] reported (Figure 3.23) the current density - V_{RE} curves of a p-InGaN alloy employed as the working electrode in the dark and UV illuminated condition. The curve in the dark condition showed comparable trend to my work, as shown in Figure 3.22. Cathodic current increased when the voltage reached -2V although their PEC cell employed Na_2SO_4 as the electrolyte which is not the identical electrolyte as we used. Therefore, the reason of these differences between our work and the work reported by K. Aryal is not clear at this point, and further investigations are required to clarify these differences.

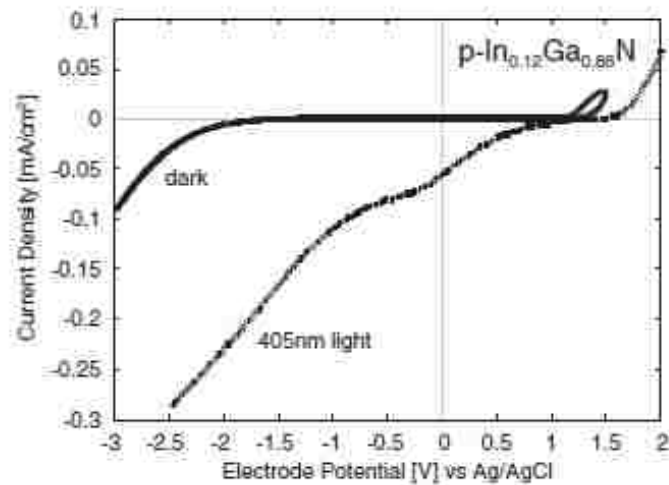


Figure 3.23. Current density - V_{RE} curves of p-InGaN in 0.1M Na_2SO_4 solution reported by S.Usui et al. [9].

3.4 Summary of the experimental work

In conclusion, solar water splitting employing n-GaN, u-GaN, p-GaN and p-InGaN alloys as the working electrode in the PEC cell were demonstrated. According to these results, our setup of the PEC cell worked normally since the current - voltage curve for the n-GaN alloy employed as the working electrode showed comparable results to that reported by S. Usui *et al.* [9], and K. Fujii *et al.* [5]. However, there was a difference between our result and the result reported by K. Aryal *et al.* [4] regarding p-InGaN and p-GaN alloys employed as the working electrode, and further investigations are still required to clarify the main factors leading to these differences.

Reference for chapter 3

- [1] Craig A. Grimes, Oomman K. Varghese and Sudhir Ranjan. *Light, Water, Hydrogen The Solar Generation of Hydrogen by Water Photoelectrolysis*. NewYork : Springer Science+Business Media, LLC, 2008: pp. 120-131.
- [2] H. P. Zhao, G. Y. Liu, X. -H. Li, R. A. Arif, G.S. Huang, J. D. Poplawsky, S. Tafon Penn V. Dierolf and N. Tansu. "Design and characteristics of staggered InGaN quantum-well light-emitting diodes in the green spectral regime." *IET Optoelectron.*, Vol. 3, Iss. 6, 2009: pp. 283-295.
- [3] J. D. Beach, R. T. Collins, and J. A. Turner. "Band-Edge Potentials of n-Type and p-Type GaN." *Journal of The Electrochemical Society*, 150 (7), 2003: A899-A904.

- [4] K. Aryal, B. N. Pantha, J. Li, J. Y. Lin, and H. X. Jiang. "Hydrogen generation by solar water splitting using p-InGaN photoelectrochemical cells." *Applied Physics Letters* 96, 2010: 052110.
- [5] Katsushi Fujii, Kazuhiro Ohkawa. "Hydrogen generation from aqueous water using n-GaN by photoassisted electrolysis." *phys.stat.sol. (c)* 3, No.6, 2006: 2270-2273.
- [6] Katsushi. Fujii, Takeshi. Karasawa, Kazuhiro. Ohkawa,. "Hydrogen Gas Generation by Splitting Aqueous Water Using n-Type GaN Photoelectrode with Anodic Oxidation." *Japanese Journal of Applied Physics Vol.44, No.18*, 2005: L543-L545.
- [7] M, Ono et al. "Photoelectrochemical reaction and H₂ generation at zero bias optimized by carrier concentration of n-type GaN." *The Journal of Chemical Physics* 126, 2007: 054708.
- [8] Mohammad Mahdi Ahmadi, Graham A. Jullien. "CUrrent-Mirror-Based Potentiostats for Three-Electrode Amperometric Electrochemical Sensors." *IEEE Transactions On Circuit and Systems, Vol. 56, No. 7*, 2009: 1339-1348.
- [9] Shogo Usui, Sadayuki Kikawa, Naoki Kobayashi, Jun Yamamoto, Yuzabaro Ban, and Kou Matsumoto. "Comparison of forward and reverse reaction in Hydrogen Generation between GaN, InGaN, Nanocrystalline TiO₂ and Pt Electrodes during Water Electrolysis." *Japanese Journal of Applied Physics Vol. 47, No. 12*, 2008: 8793-8795.

Chapter 4 : Summary and Future Work

4.1 Conclusion

The objective of this work is to set up the experimental apparatus to investigate water solar splitting employing III-nitride alloys as the working electrode of the PEC cell and to perform proof-of-concept experimental demonstration of the solar hydrogen generation with III-nitride semiconductors via solar water splitting process. The findings from this work will be valuable for the continuation of further research in this direction. This chapter is devoted to summarize the findings in this thesis, as well as to present some directions for future research works.

The basic principle of solar water splitting has been explained in chapter 2. Thermodynamically, the minimum required energy to decompose water is 1.23eV; however, in order to initiate decomposition of water, a much higher energy is required due to the overpotentials. The requirements for the semiconductor to be employed as the working electrode in the PEC cell have been presented: an appropriate band gap, proper band edge positions, and small overpotentials. The decomposition of a semiconductor alloy is also taking place when the decomposition energy levels of the semiconductor are placed inside of the band edges of the semiconductor and outside of the redox potentials. The efficiency of the PEC cell has been described, of which this definition is based on the fuel cell efficiency.

In chapter 3, the sample preparation process for the working electrodes and the experimental setup employed in this study have been described. The experimental results of solar water splitting by employing n- and p- type GaN and p-InGaN alloys as the

working electrode have been presented with comparison to those reported by others in the literature. Our results from the PEC experiments showed the hydrogen generation rate of the n-GaN working electrode samples in terms of reaction current as comparable to those reported by S. Usui *et al.* [1] and K. Fujii *et al.* [2], although there was some difference between our work and the results reported by K. Aryal *et al.* [3] for p-type semiconductor employed as the working electrode in the PEC cell. The main reasons of these differences for the p-type materials are not clear at this point.

In conclusion, our experimental setup should be enhanced to perform experiments more effectively. There are several changes that could improve the setup:

1. A sample holder to adjust position and angle of the working electrode toward the solar simulator in the PEC cell.
2. A built-in measurement instrument for the solar simulator to monitor the light intensity.
3. Additional platinum wires for the working electrodes, in order to improve the efficiency and reduce the sample preparation time.

In order to enhance the efficiency of solar water splitting, one of the key points is decrease of the overpotentials. The minimum decomposition energy cannot be decreased from 1.23eV, for that reason, decrease of the overpotential can increase reaction current. In addition, enhancement of absorption rate of photon is also key factor to increase reaction current by increasing electron-hole pairs generated by absorbed photons.

Reference for chapter 4

- [1] Shogo Usui, Sadayuki Kikawa, Naoki Kobayashi, Jun Yamamoto, Yuzabaro Ban, and Kou Matsumoto. "Comparison of forward and reverse reaction in Hydrogen Generation between GaN, InGaN, Nanocrystalline TiO₂ and Pt Electrodes during Water Electrolysis." *Japanese Journal of Applied Physics Vol. 47, No. 12*, 2008: 8793-8795.
- [2] Katsushi Fujii, Kazuhiro Ohkawa. "Hydrogen generation from aqueous water using n-GaN by photoassisted electrolysis." *phys.stat.sol. (c) 3, No.6*, 2006: 2270-2273.
- [3] K. Aryal, B. N. Pantha, J. Li, J. Y. Lin, and H. X. Jiang. "Hydrogen generation by solar water splitting using p-InGaN photoelectrochemical cells." *Applied Physics Letters 96*, 2010: 052110.

Curriculum Vitae

Takahiro Toma

Updated on: May 2011

Contact Information

11 West Second Street, Unit 348
Bethlehem, PA 18015, USA
Email: tat209@Lehigh.edu
Cell Phone: 646-496-7948

Education Background

Aug.2009-May 2011 ***Lehigh University (Bethlehem, PA, USA)***

Master of Science (M.S.) in Electrical Engineering,

- Specialization: III-Nitride semiconductors for solar water splitting
- Thesis: Proof-of-Concept Experiments of Hydrogen Generation by Solar Water Splitting by Using III-Nitride Alloys

Jun.2009-Jul.2009 ***Lehigh University (Bethlehem, PA, USA)***

English as a Second Language Program,

Apr.2002-Mar.2004 ***Ritsumeikan University (Kusatsu, Shiga, Japan)***

Master of Engineering (M.E.), emphasis on accelerator science

- Specialization: Tabletop synchrotron
- Thesis: Measurement of infrared radiation from the smallest synchrotron in the world

Apr.1998-Mar.2002 ***Ritsumeikan University (Kusatsu, Shiga, Japan)***

Bachelor of Engineering (B.E.) in Department of Photonics,

- Specialization: Tabletop synchrotron

Research/Professional experiences

Aug.2009-May 2011 ***Lehigh University (Bethlehem, PA, USA)***

Master's Thesis, MS Advisor: Prof. Nelson Tansu (Lehigh University, ECE)

Center for Optical Technologies, Electrical and Computer Engineering,

P. C. Rossin College of Engineering and Applied Science

- Set up the experimental apparatus for solar water splitting.
- Demonstrated hydrogen generation by solar water splitting employing III-Nitride semiconductor alloys.
- Assisted maintenance of MOCVD reactor and the growth of III-Nitride semiconductors for solid state lighting.

Oct.2004-Jun.2009

USHIO INC.(Harima, Hyogo, Japan)

Optical engineer

Technology & Engineering Department NSH-Business Unit Business Division 2

- Applied the optical simulation software of TracePro to company's products.
- Conducted accurate optical simulation to analyze brightness of lamp units.
- Devised a new method for designing bright reflectors for lamps.
- Technical development to dramatically reduce man-hours in operating optical simulation.

Apr.2002-Mar.2004

Ritsumeikan University (Kusatsu, Shiga, Japan)

Master's Thesis, ME Advisor: Prof. Hironari Yamada (Ritsumeikan Univ)

- Set up measurement apparatus which concentrated radiation from the synchrotron and reduced noise signal.
- Measured synchrotron radiation in infrared region from the smallest synchrotron.
- Assisted maintenance and operation of the synchrotron.

Technical Skills

- Materials Processing
 - ✓ Metal Organic Chemical Vapor Deposition (MOCVD) for Nitride Semiconductors
 - ✓ PECVD for Silicon Dioxide (SiO₂)
 - ✓ Rapid Thermal Annealing (RTA)
 - ✓ Cleanroom Process for Semiconductor Devices
 - ✓ Photo mask Design
- Analytical Tools / Techniques
 - ✓ Scanning Electron Microscopy (SEM)
 - ✓ Fourier Transform Infrared Spectroscopy (FTIR)
 - ✓ Photoluminescence (PL)
 - ✓ Gas Chromatography (GC)
 - ✓ Cyclic Voltammetry (CV)
 - ✓ Hall Measurement
 - ✓ Three-dimensional Coordinate Measuring System
- Programming Language and Software Packages
 - ✓ Visual Basic Applications
 - ✓ Mathematica
 - ✓ TracePro (optical simulation software)
 - ✓ ASAP (optical simulation software)

Patents

1. [Toma Takahiro](#), Iwabayashi Hirohisa: Light Source Device. Ushio. May, 28 2009: JP2009-117172
2. [Toma Takahiro](#), Iwabayashi Hirohisa: Light Source Device. Ushio. Apr, 16 2009: JP2009-081044
3. [Toma Takahiro](#), Horikawa Yoshihiro, Konya Wataru: Optical Device. Ushio. Oct, 9 2008: JP2008-243792
4. [Toma Takahiro](#), Horikawa Yoshihiro, Kontani Toru: Discharge Lamp With Concave Reflector. Ushio Electric. Sep, 3 2008: EP1965253 (A1)
5. [Toma Takahiro](#), Horikawa Yoshihiro, Kontani Toru: Optical Apparatus. Ushio Electric. Sep, 3 2008: CN101255973
6. [Toma Takahiro](#), Nakayama Katsuyuki, Fujii Hiroyuki, Ito Takashi: Optical System For Projector. Ushio. Jun, 26 2008: JP2008-145580
7. [Toma Takahiro](#), Nakayama Masashi, Ito Takashi, Fujii Hiroyuki: Optical System For Projector. Ushio Denki Kkjp. Jun, 16 2008: TW200825454
8. Goto Kazuhiro, Sugitani Akihiko, Terada Shoichi, [Toma Takahiro](#): Light Source Device. Ushio. Jun, 28 2007: JP2007-165067
9. Goto Kazuhiro, Sugitani Akihiko, Terada Shoichi, [Toma Takahiro](#): Light Source Device. Ushio Electric. Jun, 20 2007: EP1798752 (A1)
10. Goto Kazuhiro, Sugitani Akihiko, Terada Shoichi, [Toma Takahiro](#): Light Source Device. Ushio Electric. Jun, 20 2007: CN1983016
11. Goto Kazuhiro, Terada Shoichi, [Toma Takahiro](#), Sugitani Akihiko: Light Source Device. Ushio Denki Kkjp. Jun, 16 2007: TW200723346

Technical Refereed Journal and Conference Publications

1. **(Invited Conference Paper)** H. P. Zhao, J. Zhang, G. Y. Liu, X. H. Li, Y. K. Ee, H. Tong, [T. Toma](#), G. S. Huang, and N. Tansu, "Approaches for High-Efficiency InGaN Quantum Wells Light-Emitting Diodes – Device Physics and Epitaxy Engineering," in Proc. of the *American Vacuum Society (AVS) Meeting 2010*, Ann-Arbor, MI, May 2010.
2. **(Invited Conference Paper)** N. Tansu, H. P. Zhao, J. Zhang, G. Y. Liu, X. H. Li, H. Tong, [T. Toma](#), G. S. Huang, and Y. K. Ee, "Device Physics and Epitaxy Engineering for High-Efficiency III-Nitride Light-Emitting Diodes," in Proc. of the *International Union of Materials Research Societies - International Conference on Electronic Materials (IUMRS-ICEM) 2010*, Seoul, Korea, August 2010.
3. H. P. Zhao, J. Zhang, [T. Toma](#), G. Y. Liu, J. D. Poplawsky, V. Dierolf, and N. Tansu, "Cathodoluminescence Characteristics of Linearly-Shaped Staggered InGaN Quantum Wells

- Light-Emitting Diodes,” in *Proc. of the 23rd Annual Meeting of the IEEE Photonics Society*, Paper WY4, Denver, CO, November 2010.
4. **(Invited Conference Paper)** N. Tansu, H. P. Zhao, J. Zhang, G. Y. Liu, X. H. Li, Y. K. Ee, R. B. Song, [T. Toma](#), L. Zhao, and G. S. Huang, “Novel Approaches for High-Efficiency InGaN Quantum Wells Light-Emitting Diodes – Device Physics and Epitaxy Engineering,” in *Proc. of the SPIE Photonics West 2011, LEDs: Materials, Devices, and Applications for Solid State Lighting XV*, Paper 7954-42, San Francisco, CA, Jan 2011.
 5. H. P. Zhao, J. Zhang, [T. Toma](#), G. Y. Liu, J. D. Poplawsky, V. Dierolf, and N. Tansu, “MOCVD Growths of Linearly-Shaped Staggered InGaN Quantum Wells Light-Emitting Diodes at Green Spectral Regime,” in *Proc. of the SPIE Photonics West 2011, Gallium Nitride Materials and Devices VI*, Paper 7939-4, San Francisco, CA, Jan 2011.
 6. H. P. Zhao, J. Zhang, [T. Toma](#), G. Y. Liu, J. D. Poplawsky, V. Dierolf, and N. Tansu, “MOCVD Growths of Linearly-Shaped Staggered InGaN Quantum Wells Light-Emitting Diodes,” in *Proc. of the American Physical Society (APS) Annual March Meeting 2011*, Dallas, Texas, March 2011.
 7. **(Invited Topical Review Article)** N. Tansu, H. P. Zhao, J. Zhang, G. Y. Liu, X. H. Li, R. B. Song, L. Zhao, [T. Toma](#), and Y. K. Ee, “III-Nitride Semiconductors for Energy Applications – A Review,” *J. Phys. D: Appl. Phys.* (submitted).

Internal Scientific Seminars and Other Non-Refereed Technical Presentations

1. H. P. Zhao, G. Y. Liu, J. Zhang, [T. Toma](#), G. S. Huang, J. Poplawsky, V. Dierolf, and N. Tansu, “Enhancement of Internal Quantum Efficiency with Staggered InGaN Quantum Wells Light Emitting Diodes,” Poster Presentation in *Lehigh Nano-Energy Workshop 2010*, **Lehigh University**, Bethlehem, Pennsylvania, USA, September 2010.
2. H. P. Zhao, G. Y. Liu, J. Zhang, [T. Toma](#), G. S. Huang, J. Poplawsky, V. Dierolf, and N. Tansu, “Enhancement of Internal Quantum Efficiency with Staggered InGaN Quantum Wells Light Emitting Diodes,” Poster Presentation in *Lehigh Center for Optical Technologies (COT) Open House 2010*, **Lehigh University**, Bethlehem, Pennsylvania, USA, October 2010.